Forest Ecology and Management 358 (2015) 62–79

Contents lists available at ScienceDirect

Forest Ecology and Management

journal homepage: www.elsevier.com/locate/foreco

Mixed severity fire effects within the Rim fire: Relative importance of local climate, fire weather, topography, and forest structure

Van R. Kane [a,*], C. Alina Cansler [a], Nicholas A. Povak [b], Jonathan T. Kane [a], Robert J. McGaughey [c], James A. Lutz [d], Derek J. Churchill [a], Malcolm P. North [e]

[a] School of Environmental and Forest Sciences, University of Washington, Box 352100, Seattle, WA 98195, USA
[b] USDA Forest Service, Pacific Southwest Research Station, Institute of Pacific Islands Forestry, 60 Nowelo St., Hilo, HI 96720, USA
[c] USDA Forest Service, Pacific Northwest Research Station, University of Washington, Box 352100, Seattle, WA 98195, USA
[d] Department of Wildland Resources, Utah State University, 5230 Old Main Hill, Logan, UT 84322, USA
[e] USDA Forest Service, Pacific Southwest Research Station, 1731 Research Park Dr., Davis, CA 95618, USA

ARTICLE INFO

Article history:
Received 30 April 2015
Received in revised form 31 August 2015
Accepted 1 September 2015
Available online 8 September 2015

Keywords:
Rim fire
Spatial autocorrelation
Mixed-severity fire
Random forests
RdNBR burn severity
LiDAR
Biophysical environment
Fire history

ABSTRACT

Recent and projected increases in the frequency and severity of large wildfires in the western U.S. makes understanding the factors that strongly affect landscape fire patterns a management priority for optimizing treatment location. We compared the influence of variations in the local environment on burn severity patterns on the large 2013 Rim fire that burned under extreme drought with those of previous smaller fires for a study area in the Sierra Nevada, California, USA. Although much of the Rim fire burned during plume-dominated conditions resulting in large high-severity patches, our study area burned under milder fire weather resulting in a mix of fire severities. In our study area the Rim fire produced a higher proportion of moderate- and high-severity effects than occurred in previous fires. Random forest modeling explained up to 63% of the Rim fire burn variance using seven predictors: time since previous fire, actual evapotranspiration (AET), climatic water deficit (Deficit), previous maximum burn severity, burning index, slope position, and solar radiation. Models using only a subset of biophysical predictors (AET, Deficit, slope position and steepness, and solar radiation) explained 55% of the Rim fire and 58% of the maximum fire burn severity of previous fires. The relationship of burn severity to patterns of AET, however, reversed for the Rim fire (positive) compared to earlier fires (negative). Measurements of pre-Rim fire forest structure from LiDAR did not improve our ability to explain burn severity patterns. We found that accounting for spatial autocorrelation in burn severity and biophysical environment was important to model quality and stability. Our results suggest water balance and topography can help predict likely burn severity patterns under moderate climate and fire weather conditions, providing managers with general guidance for prioritizing fuel treatments and identifying where fire is less likely to burn with higher severities even for locations with higher forest density and canopy cover.

1. Introduction

In western North America, the frequency and severity of large wildfires is increasing (Gillett et al., 2004; Miller and Safford, 2012; Morgan et al., 2008; Westerling et al., 2006). In an effort to reduce the effects of this trend on fire-prone forests, managers prioritize areas for treatment (North et al., 2009; Hessburg et al., 2015), often based on fire model outputs (i.e., Finney, 2005). While management activities may have limited effect on large wildfires occurring during extreme fire weather, wildfires burning under more moderate weather conditions often produce a mix of burn severities where pre-fire management treatments may affect burn patterns. Previous work has shown that mixed-severity burn patterns are influenced by the local biophysical environment (Holden et al., 2009; Kane et al., 2015; Miller and Urban, 1999, 2000), but few studies have examined this in combination with pre-burn forest structure and previous fire events.

Historical reconstructions of fires (Heyerdahl et al., 2001; Taylor and Skinner, 1998) and analyses of recent fires (Cansler and McKenzie, 2014; Dillon et al., 2011; Falk et al., 2007; Kane et al., 2015; Parks et al., 2015, 2011; Prichard and Kennedy, 2014) have demonstrated the importance of both top-down and bottom-up controls (Falk et al., 2007; Heyerdahl et al., 2001; Lertzman and Fall, 1998; Perry et al., 2011). Top-down controls such as decadal,

* Corresponding author.
E-mail address: vkane@uw.edu (V.R. Kane).

http://dx.doi.org/10.1016/j.foreco.2015.09.001
0378-1127/

annual, and daily variation in precipitation and temperature influence fire similarly over large areas (Turner and Romme, 1994; McKenzie and Kennedy, 2011). Bottom-up controls such as topography create local patterns of climate and vegetation structure that influence fire by affecting fuel loading, moisture, and fire behavior (Turner and Romme, 1994; McKenzie and Kennedy, 2011). Past fires also create bottom-up controls by locally altering fuels and forest composition and structure (Collins et al., 2009; Larson et al., 2013; Peterson, 2002).

In general, bottom-up controls exert stronger influence during cooler and wetter years when fires generally burn at lower severities, while top-down controls may exert stronger influence during hotter and dryer years (Bessie and Johnson, 1995; Dillon et al., 2011; Parks et al., 2014a, 2014b; Turner and Romme, 1994). However, even in years with strong drought and warmer temperatures, the influence of bottom up controls can still be seen in some landscape burn patterns (Bigler et al., 2005; Cansler and McKenzie, 2014; Lee et al., 2009; Prichard and Kennedy, 2014; Wimberly et al., 2009).

Recent large fires in Sierra Nevada mixed conifer forests have resulted in larger patches and a higher proportion of high-severity effects than occurred historically or in contemporary smaller fires (Mallek et al., 2013; Miller and Safford, 2012; Miller et al., 2009a; van de Water and Safford, 2011). The large 2013 Rim fire (104,131 ha) occurred during an extreme drought and burned partially under extreme (>98 percentile) fire weather. However, portions of the fire burned under milder weather producing mixed-severity burn patterns for an area that also had been subject to a number of previous smaller fires. These previous fires allowed us to compare the controls on these fires to see if the controls for a large fire (the Rim fire) differed. The availability of pre-fire airborne LiDAR data over a portion of the fire allowed us to examine whether high-fidelity forest structure measurements from LiDAR would improve our ability to explain burn severity patterns.

Specifically, we examined three questions for our study area:

1. How well do local variations in climate, topography, and prior fire history explain mixed-severity burn patterns?
2. How do the effects of these controls differ for the pre-Rim fires and for the Rim fire?
3. Do pre-fire LiDAR measurements improve our ability to explain the variation?

2. Methods

2.1. Study area

Yosemite National Park (3027 km^2) lies in the central Sierra Nevada, California, USA (Fig. 1). This area has a Mediterranean climate with precipitation ranging from 800 mm to 1720 mm (Lutz et al., 2010) mostly occurring as snow during the winter. As elevation increases, mean precipitation increases, mean temperature

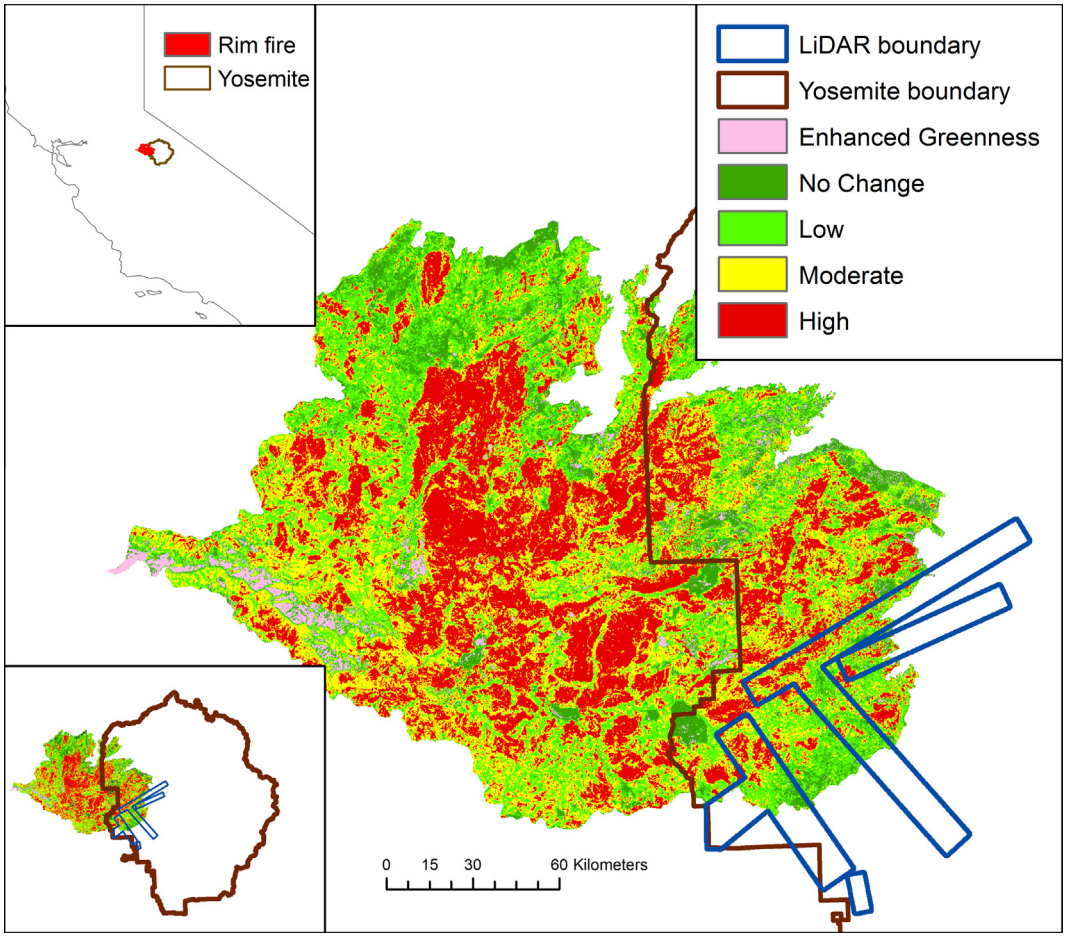

Fig. 1. Map of study area showing location within the state of California, USA (top insert) and within Yosemite National Park (bottom insert). Our study area consists of locations within the LiDAR acquisition boundary that were burned in the Rim fire. Burn severity for the Rim fire shown using classified RdNBR values with breakpoints from Miller and Thode (2007): Enhanced greenness, ⩽−150; no change detected, −150 to 68; low severity, 69–315; moderate severity, 316–640; high severity, ⩾641.

decreases, frequency of fires decreases, and mean burn intensity decreases (Lutz et al., 2010; Thode et al., 2011).

The park has multiple wildfires each year, and since 1972 many lightning-ignited fires have been allowed to burn (van Wagtendonk, 2007; van Wagtendonk and Lutz, 2007). This has resulted in most fires burning under moderate weather conditions resulting in patterns that may emulate the historic mixed-severity fire regime (Collins and Stephens, 2007; Sugihara et al., 2006a; van Wagtendonk and Lutz, 2007; van Wagtendonk, 2007). Large areas of the park have progressed towards a self-regulated fire regime (Mallek et al., 2013; van Wagtendonk, 2007; Miller et al., 2012a) with reduced fuel loads and continuity resulting in a mix of burn severities. These severities are broadly characterized as low (patches with <25% overstory tree mortality); moderate (patches with 25–75% overstory mortality); and high (patches with >75% overstory mortality) (Sugihara et al., 2006b).

To assess pre-fire forest structure we used a 5091 ha area of a 2010 LiDAR airborne acquisition that lay within the Rim fire perimeter in Yosemite spanning an elevation of 1347–2391 m. This area was a portion of the study area for three previous studies: the first two examined the effects of fire on forest structure using LiDAR data (Kane et al., 2014, 2013) and the second examined the effects of the biophysical environment on burn severity and forest structure (Kane et al., 2015).

We identified forested areas within the study area based on the 1935 and 1997 park vegetation maps (Keeler-Wolf et al., 2012; Walker, 2000; Wieslander, 1935). We excluded areas not forested in 1937 or 1997, but included areas forested in 1935 but not in 1997 based on the assumption that fire had caused a shift in vegetation type. The final study area was 4461 ha. For details on forest structure and fire history in this area see Kane et al. (2015, 2014, 2013).

Four forest types are common in the study area: ponderosa pine (*Pinus ponderosa*), sugar pine-white fir (*Pinus lambertiana–Abies concolor*), Jeffrey pine (*Pinus jeffreyi*), and red fir (*Abies magnifica*). Historically, most of these forest types were dominated by tree species with a high fire tolerance such as ponderosa pine, sugar pine, and Jeffrey pine (van Wagtendonk and Fites-Kaufman, 2006). Managers suppressed fires from the early 1900s to the early 1970s. This allowed tree species such as white fir that have lower fire tolerance when small to become established, often creating nearly continuous canopy forests with significant fuel laddering (Beaty and Taylor, 2008; Collins et al., 2011; Scholl and Taylor, 2010). When low- and mixed-severity fires burn through these forests today, ladder fuels tend to be removed, overall canopy cover is reduced, and patterns of tree clumps and openings (*sensu* Larson and Churchill, 2012; Churchill et al., 2013) can emerge (Kane et al., 2014, 2013).

2.2. Rim fire

The Rim fire started on 17 August 2013 and was not fully contained until 23 October 2013 after burning 104,131 ha of the Stanislaus National Forest and Yosemite National Park. It burned

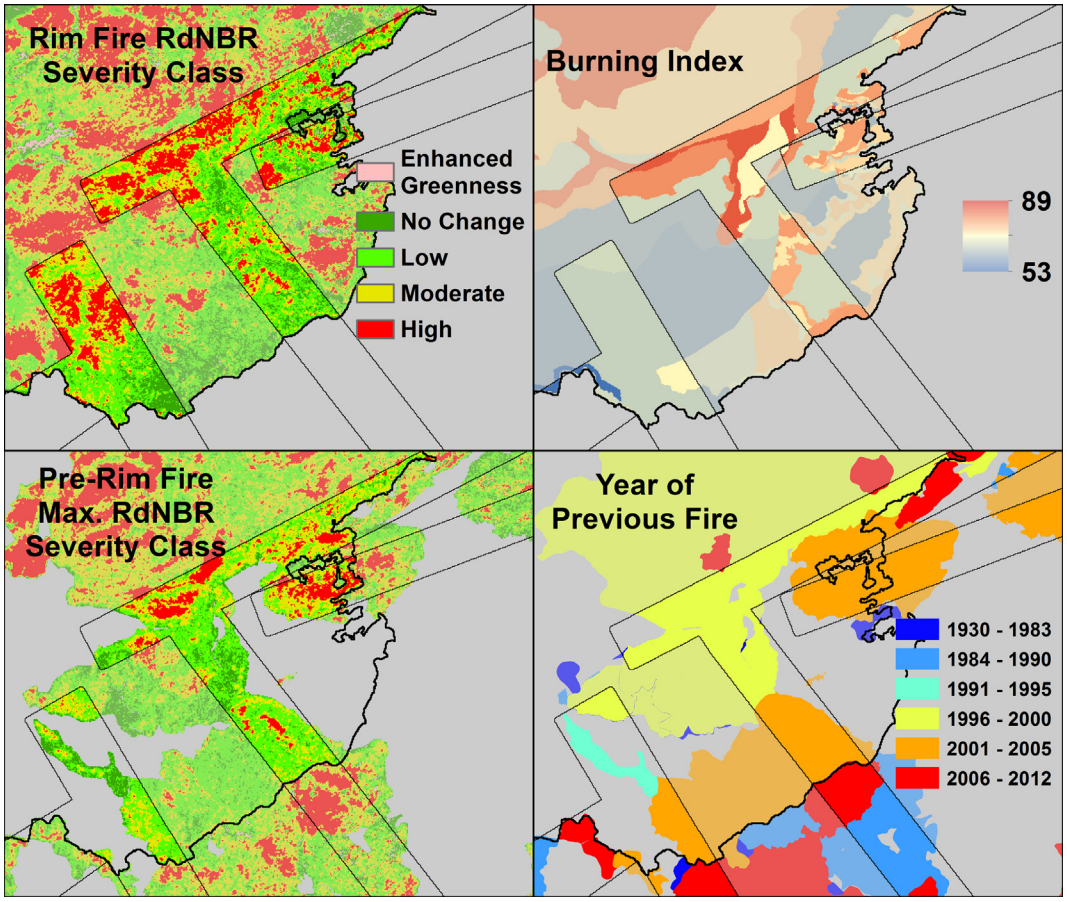

Fig. 2. Geographic variation in Rim fire estimated burn severity (RdNBR) and burn severity related predictors. Our modeling found that the burning index, a daily estimate of fire weather, the maximum RdNBR for fires prior to the Rim fire, and years since the previous Rim fire were key predictors of the Rim fire burn severity patterns. Burn severity shown using classified RdNBR values with breakpoints from Miller and Thode (2007): Enhanced greenness, $\leqslant -150$; no change detected, -150 to 68; low severity, 69–315; moderate severity, 316–640; high severity, $\geqslant 641$.

during the second year of the most extreme drought in the historical record and was the largest recorded fire in the Sierra Nevada. The Rim fire burned our study area from 26 August to 20 September 2013 and produced a mixture of burn severities (Fig. 2). Our study area burned under relatively moderate weather conditions with burning index (BI; Bradshaw et al., 1983) values predominantly in the 65–82 range, compared to the August 22 and 23 plume-dominated conditions (BI > 75) that resulted in large areas of high-severity fire effects (Lydersen et al., 2014). The southern edge of our study area was burned during fire suppression efforts by a management-ignited backfire, which we were unable to distinguish from areas burned by the Rim fire. Seventy percent of our study area had burned at least once between 1984 and 2012, allowing us to study the effects of prior fire history on the Rim fire.

2.3. Response and predictors to model burn severity

We used estimated burn severity measurements derived from Landsat images as our responses. We selected a number of predictors to test based on the work of Lydersen et al. (2014) and Kane et al. (2015) (Table 1).

2.3.1. Fire related metrics

We mapped the history of fire locations using several sources (Fig. 2). For 1930–1983 fires, we used park records of fire perimeters, excluding these areas because they lacked severity information. For 1984–2010 fires we used the Lutz et al. (2011) burn severity atlas that mapped fires ⩾40 ha. For 2011–2013 fires, we used fire maps from the MTBS project that mapped fires ⩾400 ha (Eidenshink et al., 2007).

One-year post-fire burn severities for fires from 1984 to 2013 (the earliest date for data from the Landsat Thematic Mapper instrument) were calculated using the Relativized differenced Normalized Burn Ratio, RdNBR (Miller and Thode, 2007; Miller et al., 2009b) available from the MTBS project. RdNBR estimates the effects of fire on the abiotic environment and vegetation, including the immediate impacts of the fire and ecosystem responses up to a year post-fire (Miller and Thode, 2007; Sugihara et al., 2006a, 2006b). Higher RdNBR values signify a decrease in photosynthetic materials and surface materials holding water and an increase in ash, carbon, and exposed soil. RdNBR values have been found to correlate with field-measured burn severities (Cansler and McKenzie, 2012; Soverel et al., 2010; Thode, 2005; Thode et al., 2011).

For the Rim fire, we used the continuous RdNBR values as the response. For interpretability, however, we show RdNBR in figures as classified burn severities in figures using breakpoints from Miller and Thode (2007): Enhanced greenness, ⩽−150; no change detected, −150 to 68; low severity, 69–315; moderate severity, 316–640; high severity, ⩾641. To characterize fire history in each Landsat pixel prior to the Rim fire, we used the maximum pre-Rim RdNBR value at each location and the number of years since the last fire.

We used two predictors that incorporated measures of daily weather as proxies for the Rim fire weather based on daily fire progression maps (Collins et al., 2009; Lydersen et al., 2014). The Energy Release Component (ERC) index is a measurement of fuel moisture and is calculated based on temperature, relative humidity, and related fuel moisture for 1, 10, 100, and 1000 h dead fuels, and live fuels. The Burning Index (BI) is calculated using the ERC and also includes the "spread component" which includes wind speed, slope, and live fine and woody (twigs) fuel moisture (Bradshaw et al., 1983). We used values calculated for these indices by Lydersen et al. (2014) using weather data from the Crane Flat weather station (latitude: 37.8, longitude: −119.88, elevation: 2022 m) located on the southern edge of the fire and our study area.

Table 1
Response and predictor metrics used in this study to model Rim fire burn severity. Rim fire RdNBR and pre-Rim maximum RdNBR were used as responses; all other variables were used as predictors; pre-Rim maximum RdNBR was also used as a predictor for Rim fire RdNBR. Predictors used in the parsimonious and biophysical core subsets are shown below the table. All variables were mapped using 30 m (0.09 ha) grid cells although some were calculated using larger windows around each grid cell (calculation window sizes shown in parentheses) or in the case of AET and Deficit resampled from the original 270 m rasters.

Rim fire	Source	Units/interpretation
Rim RdNBR (30 m)	MTBS[a]	Relative burn severity
Fire history (30 m)		
Time since previous fire	Park records	Years
Maximum pre-Rim RdNBR (30 m)	Lutz et al. 2011 MTBS[a]	Relative burn severity
Fire weather (daily)		
Burning index	Lydersen et al. (2014)	Relative index
Energy release component	Lydersen et al. (2014)	Relative index
Water balance (270 m/30 year averages)		
Actual evapotranspiration (AET)	Flint et al. (2013)	mm water
Climatic water deficit (Deficit)	Flint et al. (2013)	mm water
Local topography (30, 90, 270 m)		
Slope	1 m LiDAR DTM & 10 m USGS[b] DEM	Degrees
Solar radiation index (SRI)	1 m LiDAR DTM & 10 m USGS[b] DEM	Relative index
Aspect	1 m LiDAR DTM & 10 m USGS[b] DEM	Cosine (south = 0)
Slope position (100, 250, 500, 1000, 2000 m)		
Topographic position index (TPI)	1 m LiDAR DTM & 10 m USGS[b] DEM Jenness, 2006	Relative index
LiDAR forest structure (30 m)		
Cover >2, 1–2, 2–4, 4–8, 8–16, 16–32, >32 m	LiDAR	Percent
>2 m return height percentiles: 10th, 25th, 50th, 75th, 95th	LiDAR	Meters
Standard deviation return heights >2 m	LiDAR	Meters
Rumple (canopy surface rugosity)	LiDAR	Ratio

Parsimonious predictors: AET, Deficit, pre-Rim max. RdNBR, time since previous fire, slope position (1000 m), solar radiation index (270 m), slope (270 m), burning index.
Biophysical core predictors: AET, Deficit, slope position (500 and 1000 m), solar radiation index (270 m), slope (270 m).
[a] Monitoring Trends in Burn Severity.
[b] United States Geological Survey.

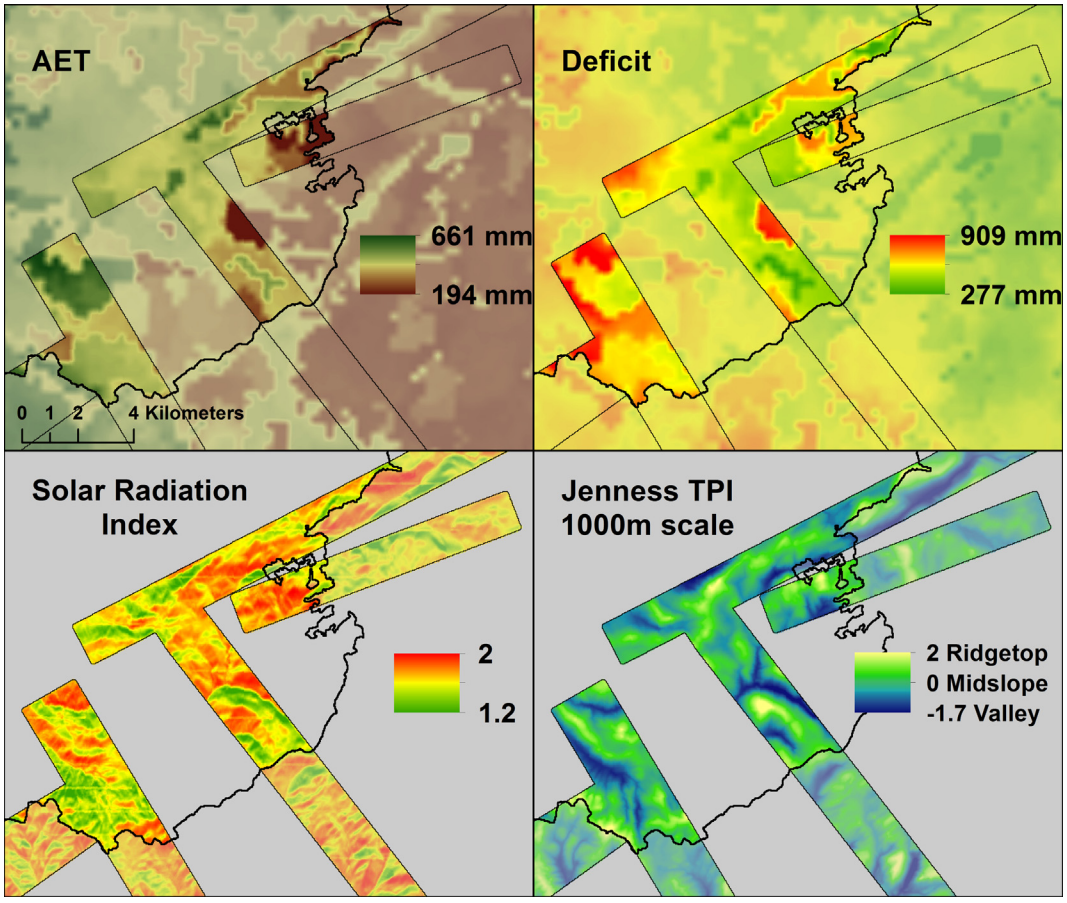

Fig. 3. Geographic variation in biophysical environmental conditions that our modeling found to be key predictors for the burn severity patterns for both the Rim fire and previous fires. Actual evapotranspiration (AET) and climatic water deficit (Deficit) are surrogates for patterns of local potential productivity and fuel accumulation and for fuel moisture. The solar radiation index integrates slope, aspect, and latitude into a measure of relative solar exposure based on topography. The Jenness Topographic Position Index (TPI) indicates relative slope positions.

2.3.2. Pre-Rim fire LiDAR data and forest structure metrics

LiDAR data were collected by Watershed Sciences, Inc. (Corvallis, OR) using dual mounted Leica ALS50 Phase II instruments. Data were collected on 21 and 22 July 2010 with an average pulse density of 10.9 pulses m^{-2} with up to four returns per pulse. Watershed Sciences created a 1 m resolution LiDAR-derived digital terrain model (DTM) using the TerraScan (v.10.009 and v.11.009) and TerraModeler (v.10.004 and v.11.006) software packages (Terrasolid, Helsinki, Finland).

We processed the LiDAR data using the USDA Forest Service's Fusion software package (beta version derived from version 3.4.2, http://forsys.cfr.washington.edu/fusion.html) (McGaughey, 2014). We produced a set of forest structure metrics using a 30 m (0.09 ha) grid. Metrics for the distribution of the canopy profile were calculated as the heights at which a percentile of returns (e.g., 25th percentile height) >2 m occurred. We measured the structural heterogeneity of the forest canopy by calculating the standard deviation of return heights >2 m and with a measure of canopy rugosity, rumple, calculated from a canopy surface model (CSM) created using the maximum return height within each 1-m grid cell smoothed with a 3 × 3 low pass filter. Canopy cover was calculated as the percentage of returns in a stratum divided by the number of returns in that stratum and all lower strata for strata >2, 1–2, 2–4, 4–8, 8–16, 16–32, and >32 m.

2.3.3. Water balance metrics

In mountainous areas, potential fuel biomass and dryness are related to elevation gradients associated with differences in precipitation and temperature. While many studies have used elevation as a predictor (Holden et al., 2009; Prichard and Kennedy, 2014), several have used water balance to integrate the simultaneous availability of water and energy (Abatzoglou and Kolden, 2013; Kane et al., 2015; Littell and Gwozdz, 2011; Parks et al., 2014a, 2014b).

The theoretical limit to plant photosynthesis is correlated with potential evapotranspiration (PET), which is based on available energy. However, photosynthesis is limited by water availability, so the actual evapotranspiration (AET) is less than the PET when not enough water is available to meet evaporative and transpiration demands. The difference between PET and AET is the climatic water deficit (Deficit, *sensu* Stephenson (1998)), which estimates vegetation stress due to lack of water. AET is associated with potential biomass and hence potential surface fuel deposition while Deficit is correlated with fuel moisture and hence fire behavior (Kane et al., 2015; Miller and Urban, 1999). AET and Deficit are correlated to the elevation gradient through patterns of precipitation (higher elevations generally receive more) and temperature (higher elevations are colder) leading to water-limited forests at lower elevations and energy-limited forests at higher elevations (Das et al., 2013; Greenberg et al., 2009).

We used AET and Deficit 270 m scale maps resampled to 30 m from the 2011 California Basin Model (BCM) (Flint and Flint, 2007; Flint et al., 2013, http://climate.calcommons.org/dataset/10) that used a Priestley–Taylor (Priestley and Taylor, 1972) PET model with a Thornthwaite–Mather (Thornthwaite and Mather, 1955) style AET and deficit model (Fig. 3).

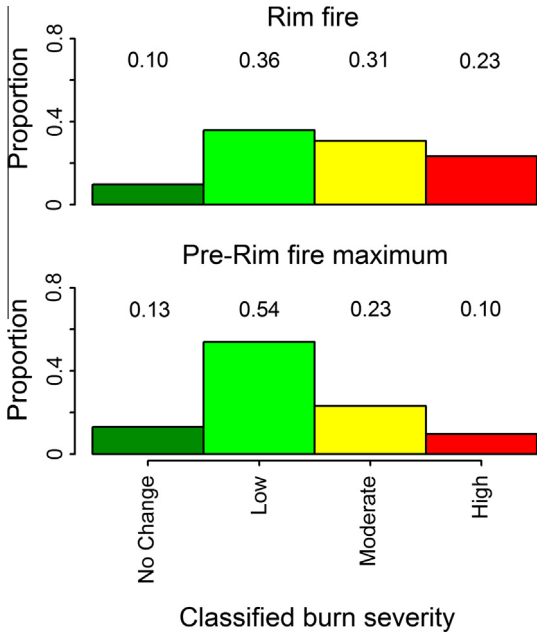

Fig. 4. Proportion of study area that burned at different RdNBR classified burn severities for our study area in the 2013 Rim fire and pre-Rim fires from 1984 and 2012. Burn severity shown using classified RdNBR values with breakpoints from Miller and Thode (2007): Enhanced greenness, $\leqslant -150$; no change detected, -150 to 68; low severity, 69–315; moderate severity, 316–640; high severity, $\geqslant 641$.

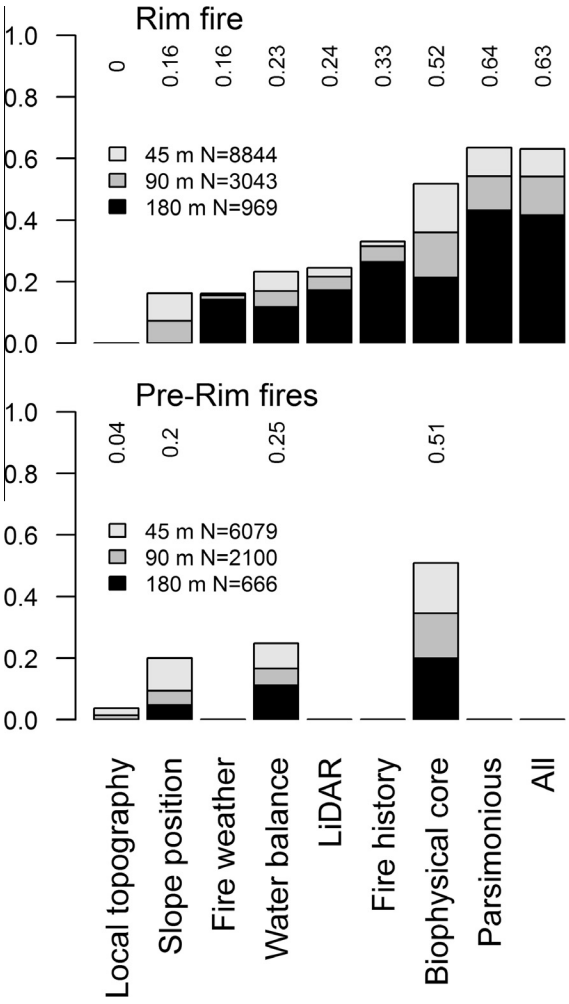

Fig. 5. Variance explained for the 2013 Rim fire burn severity (top) and pre-Rim fires (bottom) using different categories of predictors for different sample spacings. Numbers above each bar show variance explained for a sample spacing 45 m. Predictors within each category are listed in Table 1.

2.3.4. Topographic metrics

We evaluated the effects of topography on burn severity using several metrics. Topographic metrics are calculated based on terrain within a given area. We could not know a priori what scales would best correlate with fire behavior as measured by burn severity so we calculated each metric at multiple scales. The calculations were done using a moving window analysis. For example, starting with the center point of each grid cell, we measured slope at scales of 30 m, 90 m, and 270 m for the area surrounding each grid cell. Within the area of the LiDAR acquisition, we used the LiDAR-derived 1 m digital terrain model (DTM). To calculate these metrics at the edge of the LiDAR extent, values from the 10 m US Geological Survey digital elevation model were used when points in the analysis window fell outside of the LiDAR-derived DTM. Calculations were done using a software tool that is planned for release in a future version of the Fusion software (McGaughey, 2014).

We calculated slope, aspect, and a solar radiation index (SRI) for scales of 30 m, 90 m, and 270 m. The software used a 3×3 grid of points spaced at half the distance of the scales examined to calculate the slope and aspect (Zevenbergen and Thorne, 1987). SRI distills information about slope, aspect, and latitude into a single linear value useful for comparing relative solar radiation loads across a study area (Fig. 3). SRI models solar radiation during the hour surrounding noon on the equinox (Keating et al., 2007):

$$\mathrm{SRI} = 1 + \cos(\mathrm{latitude}) \times \cos(\mathrm{slope}) + \sin(\mathrm{latitude}) \times \sin(\mathrm{slope}) \times \cos(\mathrm{aspect}) \quad (1)$$

where latitude and slope are in degrees and aspect is relative to south.

We calculated slope positions using annuli of 100 m, 250 m, 500 m, 1000 m, and 2000 m radii using an algorithm that replicates the Topographic Position Index (TPI; Jenness, 2006; Weiss, 2001) (Fig. 3). More negative TPI values indicate a position towards a valley bottom, values near zero indicate flat areas or mid-slope, and more positive values indicate a hill or ridge top.

Preliminary analysis showed that burn severity was more strongly correlated with slope position than with the other topographic metrics. We therefore report slope position results separately from slope, aspect, and SRI, which are collectively referred to as 'local topography'.

2.4. Modeling for Rim fire burn severity

2.4.1. Random forest models

We used the random forest supervised learning algorithm (Breiman, 2001; Cutler et al., 2007) because it can find complex relationships between predictors and response, minimizes overfitting of data sets, and can accept spatial autocorrelation in predictor data (Breiman, 2001; Cutler et al., 2007). This modeling is an extension of non-parametric classification and regression trees (CART; Breiman et al., 1984) developed to reduce the overfitting of data common with CART models. A CART model recursively partitions observations into statistically more homogeneous groups based on binary rule splits on the predictor variables, which can be categorical or continuous. CART models deal effectively with non-linear relationships between predictor and response variables, interactions between predictors, and impose no assumptions on the distribution of the response or predictor variables.

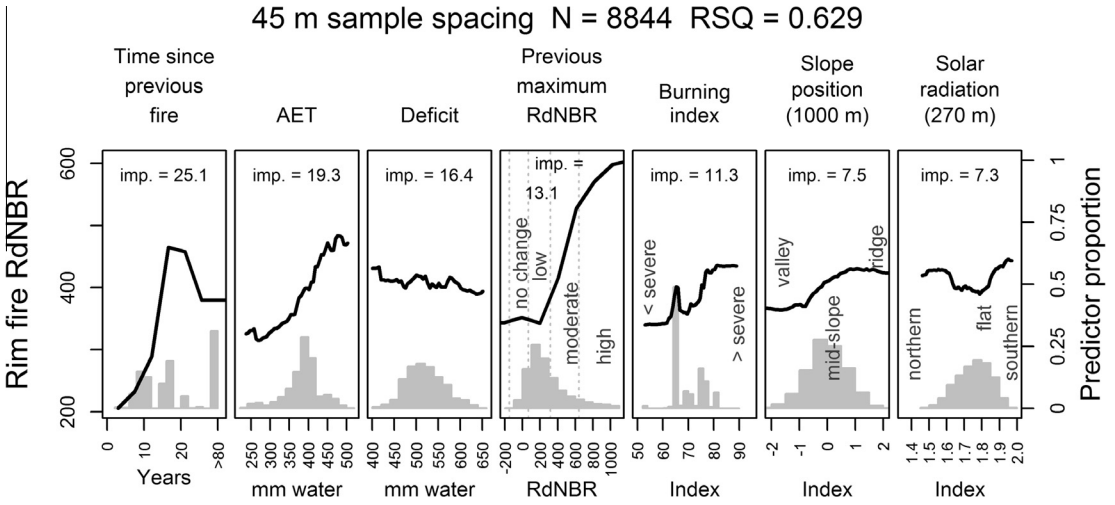

Fig. 6. Partial plots showing relationships between each of the predictors in the parsimonious predictor set and the 2013 Rim fire burn severity (RdNBR) from random forest modeling. Number within each panel shows the normalized importance of each predictor in the model ("imp. ="). Variance explained by model shown as a pseudo R^2 ("RSQ ="). Solid lines show trends in RdNBR in response to each predictor (left scale) while histograms show the distributions of values for each predictor (right scale). Model trends where there are few samples at extreme values for predictors should be treated with caution. For predictors that are index values, interpretative text is included within each panel. Relationships between each predictor and the response (RdNBR) calculated as partial dependence plots where the values for each predictor are varied throughout their range while values for all other predictors are held to their mean values. As a result, partial dependence plots do not show interactions between predictors. Partial plots for other sample distances shown in Appendix A.

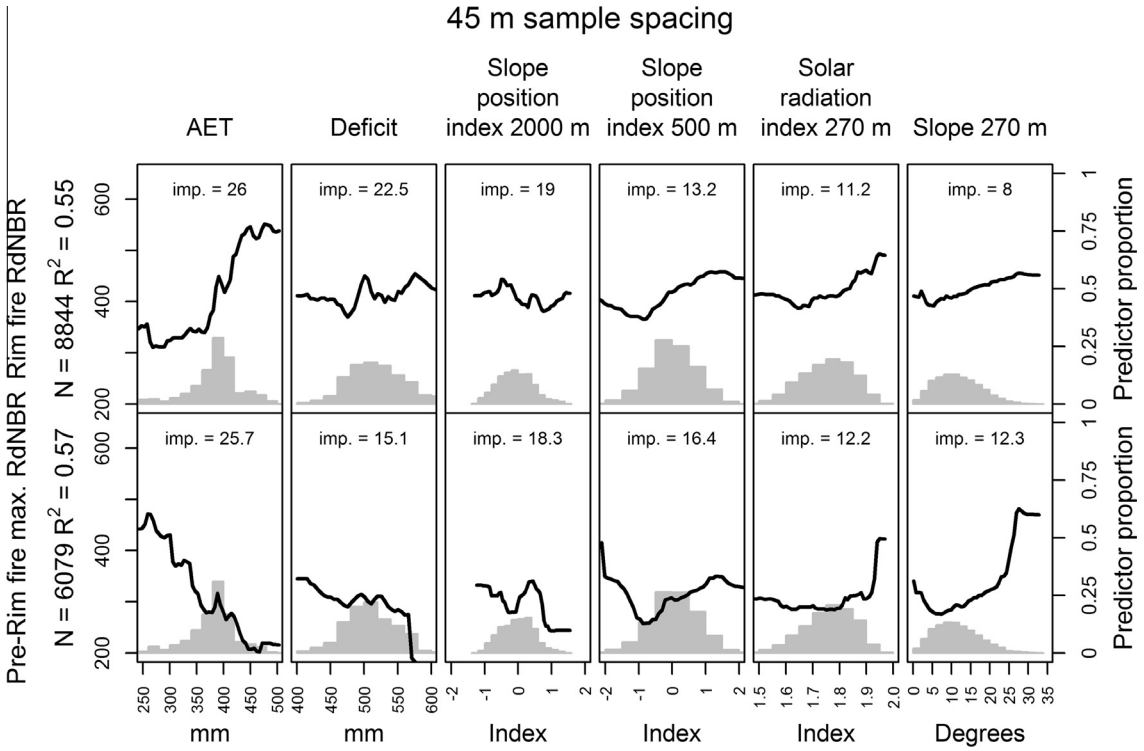

Fig. 7. Relationships between each of the predictors in the biophysical core predictor set and the 2013 Rim fire and pre-Rim fire burn severities (RdNBR) as modeled by random forest modeling. The key difference between the Rim fire and pre-Rim fires are in the relationships between AET burn severities. Number within each panel shows the normalized importance of each predictor in the model ("imp. ="). Variance explained by model shown as a pseudo R^2 ("RSQ ="). Solid lines show trends in RdNBR in response to each predictor (left scale) while histograms show the distributions of values for each predictor (right scale). Model trends where there are few samples at extreme values for predictors should be treated with caution. For predictors that are index values, interpretative text is included within each panel. Relationships between each predictor and the response (RdNBR) calculated as partial dependence plots where the values for each predictor are varied throughout their range while values for all other predictors are held to their mean values. As a result, partial dependence plots do not show interactions between predictors. Partial plots for other sample distances shown in Appendix A.

Random forest models develop "forests" of CART trees to deal with the overfitting common with single CART models. For each CART model, a random portion of the data is selected to train the model (bagging) and the remaining data are used for model validation (i.e., out-of-bag or generalization error). Random subsets of predictors are selected at each node split to ensure that the effects of all predictors are tested.

Variance explained is equivalent to the coefficient of determination (R^2) for linear regressions and reports how well a statistical model fits a given dataset. Random forest variance explained can

be calculated using either the internal out-of-bag error rate, or by predicting to a separate independent validation sample. We report the variance explained based on internal out-of-bag error rates after confirming that there was almost no difference between the methods.

We report the normalized importance of each predictor to the variance explained by a model that is calculated by randomly permutating out-of-bag values for each predictor. The resulting change in mean square error from the original out-of-bag data is used to calculate the variable importance measure. We used partial dependence plots (Hastie et al., 2001) to examine the relationship of individual predictors to burn severity.

2.4.2. Models evaluated

To identify the key drivers of the Rim fire burn severity, we selected a parsimonious subset of predictors that explained approximately 95% or more of the variance explained by the full set of predictors: Years since previous fire, maximum pre-Rim fire RdNBR, AET, Deficit, BI, SRI at 270 m scale, and slope position at 1000 m scale. We selected this subset by starting with the predictor reported as most influential from the run with all predictors and then testing the addition of all remaining predictors one at a time to see which best improved modeling results given previously selected parsimonious predictors. We iteratively repeated this process using previously selected predictors until no additional predictors improved variance explained by more than 2%.

We also wanted to compare the ability to explain patterns of burn severity based only on the biophysical environment and then also with fire history and fire weather as additional predictors. We searched for a minimum set of biophysical predictors, and found the same set that had been identified by Kane et al. (2015) using similar methods to ours: AET, Deficit, slope position index at 500 and 2000 m scales, and slope and solar radiation at 270 m scales. We ran models using this set of biophysical core predictors to allow us to determine how much burn severity was attributable to a set of biophysical conditions alone compared to these plus other types of predictors. Reporting these results also allows our results to be directly compared with those of Kane et al. (2015).

We modeled the Rim fire estimated burn severity (RdNBR) using all predictors and separately using subsets of predictor categories: the parsimonious, biophysical core, LiDAR forest structure, local topography, slope position, pre-Rim fire history, and water balance predictors (Table 1). Developing multiple models allowed us to explore the importance of different subsets of controls on patterns of burn severity. To test whether the Rim fire interacted differently with the landscape pattern than previous fires had, we modeled the maximum pre-Rim fire burn severity at each location for fires from 1984 to 2012.

2.4.3. Sample size and spatial autocorrelation

We tested for spatial autocorrelation within our data sets and results using spatial correlograms of the Moran's *I* coefficient (Legendre and Legendre, 2012) and found that burn severity and most of our predictors showed strong spatial autocorrelation at scales <1000 m (Appendix A). Parametric techniques, such as linear modeling, require that samples not be spatially autocorrelated. Consequences of spatial autocorrelation on parametric models include inflated significance of predictor variable coefficients (i.e., inflated Type I error-rates), bias towards the selection of certain environmental predictors due to their inherent spatial structure, and "red-herrings" in the interpretation of important drivers of ecological processes (Clifford et al., 1989; Lennon, 2000). However, implications of spatial autocorrelation on non-parameteric models are less clear as variable importance is not assessed based on statistical significance. We tested spatial autocorrelation with systematic sampling using different minimum spacing distances between samples (45 m ($N = 8844$), 90 m ($N = 3034$), 180 m ($N = 969$), 360 m ($N = 287$), and 720 m ($N = 85$). A minimum sample spacing of 45 m prevented adjacent samples. We provide full details of our methods to test for spatial autocorrelation in Appendix A.

3. Results

Based on our analysis of spatial autocorrelation, we found that sample spacing distances of 45 m and 90 m and to a lesser degree 180 resulted in stable models that showed consistency between burn severity and our predictors and differed primarily in the variance explained (Appendix A). Models generated with sample spacing distances of 360 m and 720 m produced unstable sets of parsimonious predictors between runs with same sample sets, oscillating patterns of spatial autocorrelations in the model residuals, and poor variance explained ($R^2 < 0.28$). Models with all tested spacing distances had some spatial autocorrelation in the residuals, but substantially less than in the RdNBR burn severity patterns and the predictors. We therefore report summary results for the 45 m, 90 m, and 180 m spacing distances (Fig. 5) and more detail for the 45 m spacing to report highest model fidelity (Figs. 6 and 7). Detailed results of our spatial autocorrelation analysis and full results for all sample spacing distances are reported in Appendix A.

A higher proportion of the study area burned at moderate- and high-severity in the Rim fire than for previous fires (Fig. 4). A parsimonious set of seven predictors (Table 1 and Figs. 5 and 6) explained 41–63% of the variance depending on sample spacing, the same range as for all predictors (sample spacing distances of 45 m, 90 m, and 180 m). The biophysical core predictors (Table 1 and Fig. 7) explained almost the same amount of burn severity variance for the Rim fire and previous fires.

We found that the relationship of AET with burn severity changed between the pre-Rim fires and the Rim fire (Fig. 7). For pre-Rim fires, higher AET values were correlated with lower burn severities while this relationship reversed for AET with the Rim fire. Deficit as a standalone predictor did not have a clear relationship with burn severity for the Rim fire or previous fires and only had a clear relationship with pre-Rim burn severity at extreme Deficit values. When Deficit was experimentally dropped from the biophysical predictor set, burn severity variance explained dropped from 52% to 34% for the Rim fire and from 51% to 37% for previous fires (45 m sample spacing distance). This indicated that Deficit alone provides some information to explain burn variance not provided by other predictors, but Deficit influences burn severity in combination with one or more other predictors (which the partial plots in Figs. 6 and 7 cannot show).

4. Discussion

We found that in the portion of the Rim fire examined in our study area, a substantially larger proportion of the area burned at moderate and high severities than for the previous smaller fires. Variations in burn severity for both previous fires and the Rim fire were best explained using predictors for water balance, slope position, and local topography. For the Rim fire, also incorporating previous fire history and fire weather metrics modestly improved results. We were surprised to find that pre-fire LiDAR measurements of forest structure did not improve our ability to explain Rim fire burn severity patterns. We discuss the implications of spatial autocorrelation among fire severity, our predictors, and in our models in Appendix A.

4.1. Predictors of fire severity for Rim and pre-Rim fires

The proportion of our study area that burned at moderate (31%) and high (23%) severities during the Rim fire was substantially greater than for the maximum burn severity of previous fires (23% and 10%, respectively) (Fig. 4). The Rim fire burned in the second year of a severe drought with fuels likely drier than normal, and large fires are more likely in years with low spring snow packs (Lutz et al., 2009). This is consistent with the observation that large fires such as the Rim fire burn at higher average severity than smaller fires even when fire weather is not extreme (Cansler and McKenzie, 2014; Lutz et al., 2009; Miller and Safford, 2012; Miller et al., 2012b, 2009a; van Wagtendonk and Lutz, 2007). This annual climate condition was likely a top-down control on Rim fire burn severity.

Burn severity patterns appear to reflect the influence of a range of conditions rather than dominance by any single one. In testing the six categories of predictors, we found that the variation explained by any single category ranged from none (local topography) to a third (fire history) but combining predictors from across categories improved variance explained to almost two thirds (Fig. 5). A subset of six biophysical predictors (AET and Deficit, slope position, slope, and solar radiation index) performed nearly as well as all predictors (Figs. 5 and 7). Adding fire history (time since previous fire and maximum prior burn severity (RdNBR)) and an index of daily fire weather only modestly improved results achieved using the biophysical predictors, which supports the previously identified importance of the biophysical environment (Miller and Urban, 1999, 2000; Kane et al., 2015).

Two other studies used pre-Rim fire field data that examined predictors of the Rim fire's mixed-severity burn patterns found a similar core set of influential predictors but with some differences. Among biophysical predictors, Lydersen et al. (2014) and Harris and Taylor (2015) found elevation (strongly correlated with AET and Deficit within the scale of our study area) to be a strong predictor, while Harris and Taylor found slope position important (which Lydersen et al. did not test). Our study and Harris and Taylor's found that time since previous fire to be an important predictor, and Lydersen et al. found the burning index to be important but Harris and Taylor did not. The other two studies found pre-fire shrub cover (Lydersen and North, 2012; van Wagtendonk et al., 2012) to be an important predictor, but the ability of LiDAR data to reliably measure shrub cover over large areas hasn't been demonstrated, and we did not test this.

The predictors for previous fire history explained a third of the Rim fire burn severity when considered alone. However, the parsimonious predictor set, which includes both prior fire history and biophysical predictors, explained just 11% more of the burn severity pattern than the biophysical core subset that did not include prior fire history predictors (45 m sample spacing) (Fig. 5). While the behavior of mixed-severity fires is often seen to have a substantial stochastic element based on weather during the year and days of the fire (Halofsky et al., 2011; Perry et al., 2011), much of the past fire history in our study area appears to be correlated with the biophysical conditions (Kane et al., 2015; Miller and Urban, 1999). As a result, prior fire history cannot be viewed as a fully independent variable separate from the biophysical environment. The relationship between the biophysical environment and fire severity could be one reason why repeat fires often tend to burn with similar burn severities at each location (Lydersen and North, 2012; van Wagtendonk et al., 2012).

We found that the relationship between burn severity and AET changed substantially between the Rim fire and pre-Rim fires (Fig. 7). AET is a surrogate for productivity, and therefore the potential quantity of live fuels (Kane et al., 2015; Mu et al., 2007) and the surface fuels that are shed from living and dead biomass (Miller and Urban, 2000; van Wagtendonk and Moore, 2010). For pre-Rim fires, higher AET 30-year normal values were negatively correlated with burn severity, which is consistent with higher AET being found in areas with increased precipitation and later snow melt and therefore usually having wetter fuels during the fire season (Miller and Urban, 1999, 2000). However, for the Rim fire, higher AET values were positively correlated with higher burn severities. One explanation might be that the drought present during the Rim fire dried locations that usually had higher fuel moistures, and the Rim fire burned the fuel accumulations that had built up in these areas (Miller and Urban, 2000). This would suggest that at least two relationships can exist between water balance and burn severity patterns, varying with the actual climate during the year of a fire. Schoennagel et al. (2005) found a similar relationship in the Rocky Mountains.

Fire weather incorporates inter-annual, day to day, and minute-to-minute variations in weather and is a major factor influencing the frequency and severity of fires (Halofsky et al., 2011; Lutz et al., 2009; Perry et al., 2011). The only surrogates for fire weather available were estimates based on daily weather (BI and ERC), which could not capture intra-day or spatial variability in weather. We found that using our fire weather predictors only modestly increased burn severity predictions. By the time the Rim fire reached our study area, BI variability was limited (65–82). For areas that burned earlier in the fire Lydersen et al. (2014) found BI to be a more significant predictor for the Rim fire burn severity than we did when they examined its behavior over a wider range of burning index values for both days with plume and non-plume dominated weather. The importance of weather, therefore, for predicting the burn severity of a fire is likely to vary from fire to fire and during a single fire based on the range of fire weather experienced.

4.2. Lack of predictability from LiDAR measurements

We had hypothesized that much of the Rim fire burn severity patterns reflect previously unmeasured patterns of surface fuels and shrub cover. We therefore expected that high-fidelity forest structure measurements from LiDAR at 30 m scale would more accurately reflect local conditions than modeled water balance estimates mapped at 270 m scale, which serve as a surrogate for potential biomass and fuels. Similarly, we expected that measured forest structure would more accurately reflect the effects of past burns than the estimated burn severity from Landsat spectral measurements. However, the biophysical, fire history, and fire weather predictors used together better explained burn severity patterns (Fig. 6).

We see two explanations for these results. First, LiDAR measures overstory forest structures that are only poorly correlated with surface fuels (Jakubowksi et al., 2013; Keane et al., 2012a, 2012b; Lydersen et al., 2015). Second, fine-scale fuel patterns may not predict burn severity patterns well. Lydersen et al. (2014) and Harris and Taylor (2015) used pre-Rim fire fuel data from plot networks covering portions of the burned area, and they found weak relationships between pre-fire fuels and Rim fire burn severity. Burn severity patterns vary at larger scales than the 0.1 ha field plots used in these studies and our 0.09 ha LiDAR metric grid cells. The larger scales represented by our biophysical predictors may simply better match the scales at which fire behavior, the biophysical environment, and fuel variations correlate.

4.3. Management Implications

We found that the biophysical template and past fire history can have a significant influence on mixed-severity burn patterns in this large fire. Our results are consistent with the findings of

others for fires under a variety of climatic conditions (Cansler and McKenzie, 2014; Collins et al., 2007, 2009; Dillon et al., 2011; Gill and Taylor, 2009; Holden et al., 2009; Kane et al., 2015; Lydersen et al., 2014; Miller and Urban, 1999; Parks et al., 2011, 2012, 2014a, 2014b; Prichard and Kennedy, 2014; Wimberly et al., 2009).

Managers could use this knowledge to manage forested landscapes to promote patterns of forest structure that are likely to persist through future fires and maintain key species (see also Miller et al., 2012b; Smith et al., 2014). For example, stands of higher canopy cover supporting sensitive species (e.g., the fisher (*Martes pennanti*) and California spotted owl (*Strix occidentalis occidentalis*)) that are likely to experience lower fire severities (e.g., locations with higher AET, toward valley bottoms, and burned with lower severities previously) might be a lower priority for fuels reduction treatments. Conversely, stands in areas more likely to burn with higher severities (e.g., locations with lower AET, toward ridge tops, and burned with higher severities previously) might become a priority for significant fuels reduction, or stands surrounding them might be treated to create buffers to moderate fire severities. A warning, however, for these general principles is that we found likely burn severity may "flip" during the extensive drying of severe droughts, producing higher severities in areas that are normally moister (higher AET, lower Deficit). Management strategies built on burn severity estimates for both normal and more extreme conditions will be more robust. For example, retaining or creating some more open forest patches in settings that typically would burn at lower severities should create more resilient landscapes.

In our study, as in others (Parks et al., 2014a, 2014b; Thompson et al., 2007; van Wagtendonk et al., 2012) low- and high-severity fire appears to beget more of the same severity. While the former is desirable, if patterns of high-severity fire become entrenched, large portions of forests may become locked into cycles of repeat high-severity fires. To prevent this pattern, wider use of prescribed burns and managed wildfire under moderate weather conditions may help perpetuate variable fire effects in subsequent burns. Outside of National Parks and Wilderness areas, mechanical fuels reduction may also reduce burn severity in areas that are accessible and economic for machine-based treatment (North et al., 2015).

Improving predictive models of burn severity based on the methods of this and related studies (e.g., Miller and Urban 1999; Holden et al., 2009) will reduce the uncertainty and risk that managers face when using both prescribed fire and managed wildfire. A useful next step would be for researchers to develop models that predict likely ranges of burn severity across landscapes given the biophysical template and past fires. These model results could be used in conjunction with process based fire spread models (e.g. Flammap) to better identify settings that are more likely to burn at low, moderate, or high severity under a range of climatic and fire weather scenarios.

Acknowledgements

We thank two anonymous reviewers for their helpful comments. Jamie Lydersen provided the burning index and energy release component data used in this study. Lorraine E. Flint and Alan L. Flint provided AET and Deficit data from their California Basin Characterization Model. Funding for this research was provided by the U.S. Forest Service grants 13·CS-11052007-055 and 14-JV-11272139-014. Funding for the acquisition of the LiDAR data was provided by the National Park Service, Fire and Aviation Management Branch, Fuels and Ecology Program (Interagency Agreement F8803100015) and the U.S. Geological Survey Terrestrial, Freshwater, and Marine Ecosystems Program. Any use of trade, product, or firm names is for descriptive purposes only and does not imply endorsement by the US Government.

Appendix A. Random forest results and spatial autocorrelation

A.1. Background

Spatial autocorrelation (SA) describes the relationship between pairs of observations that are more similar (positive correlation) or less similar (negative) than would be expected by random based purely on their spatial proximity to one another (Legendre, 1993). SA is described informally by Tobler's first law of geography where he states "...near things are more related than far things" (Tobler, 1970). Spatial autocorrelation among variables is an inherent and important aspect of ecological variables responsible for observed landscape patterns, patches, and gradients that are the focus of much study in ecology.

The implications of SA on ecological modeling have been the focus of debate (Dubin, 1998; Diniz-Filho et al., 2003; Dormann et al., 2007; Hawkins et al., 2007). The presence of SA violates the assumption of independence among observations. For parametric models, SA is known to narrow confidence intervals around coefficient estimates, which can inflate their significance. However, for nonparametric regression models, such as the random forest model used in our study, it is less clear what the direct influences of spatial autocorrelation are on model structure, model predictions, and variable importance measures (though see, Hothorn et al., 2011).

In this appendix, we first examine the spatial autocorrelation in burn severity, predictors, and residuals. We then repeat key analyses from our paper using several minimum sample spacing distances of 45, 90, 180, 360, and 720 m that were chosen to reduce fine-scale spatial autocorrelation in the residuals.

We used correlograms (Moran's I coefficient (Legendre and Legendre, 2012)) to assess the level of SA in model prediction residuals, Rim Fire RdNBR response variable and parsimonious model predictor variables at sample points across a variety of distance intervals. The Moran's I was calculated among points within 42.4 m distance classes (i.e., equal to the diagonal distance among 30 m cells (42.4, 84.9, 127.3, 169.7 m, etc.)). Correlograms were calculated using the ncf package within the R statistical package. Moran's I values range from −1 (dispersed) to 1 (clustered), with 0 indicating random spatial pattern.

A.2. Spatial autocorrelation in burn severity, predictors, and residuals

Rim fire RdNBR (response) and most of our predictors showed strong spatial autocorrelation across one to two orders of magnitude of spatial scales (Fig. A1). RdNBR exhibited SA mainly between 30 and 2500 m. For distances >2500 m, RdNBR SA oscillated around zero, with a slightly dispersed pattern identified between 5000 and 12,000 m.

We found a high level of SA in the predictor variables used in the parsimonious model (Fig. A1). With the exception of topographic position index (TPI), positive correlations existed generally between 30 and 5000 m, after which an inhibitory SA relationship was identified. TPI exhibited a clustered pattern from 30 to 500 m. A surprising result was that the predictors 'time-since-last-fire' and 'Pre-Rim RdNBR' had similar correlogram signatures as the AET and Defiict, possibly suggesting a further link between the biophysical environment and fire severity and frequency.

SA was identified in the out-of-bag residuals resulting from the parsimonious random forest model for all sample spacing distances (Fig. A2). The largest positive (clumped distribution) SA existed between 30 m and 300 m, although some positive Moran's I values were found at larger distance intervals. Moran's I values were substantially lower for model residuals compared to the response variable Rim Fire RdNBR.

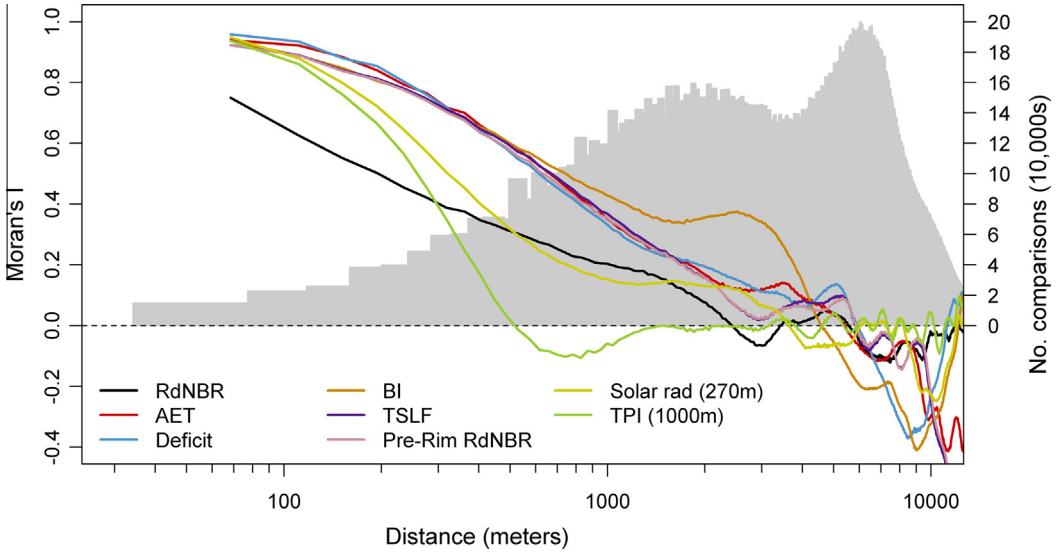

Fig. A1. Moran's *I* correlogram on Rim RdNBR response variable, and predictor variables used in the parsimonious model using a sample spacing of 42 m to allow adjacent samples. Gray bars indicate the number of unique interactions among pairs. RF model was built using 8844 random samples spaced at a minimum distance of 45 m. Note the *x*-axis is in log10 distance units. Moran's *I* values range from −1 (dispersed) to 1 (clustered), with 0 indicated completely random. The abbreviations are RdNBR, Relativized differenced Normalized Burn Ratio; AET, Actual Evapotranspiration; Deficit, climatic water Deficit; BI, Burning Index; TSLF, Time Since Last Fire; Solar rad, Solar radiation index; and TPI, Topographic Position Index.

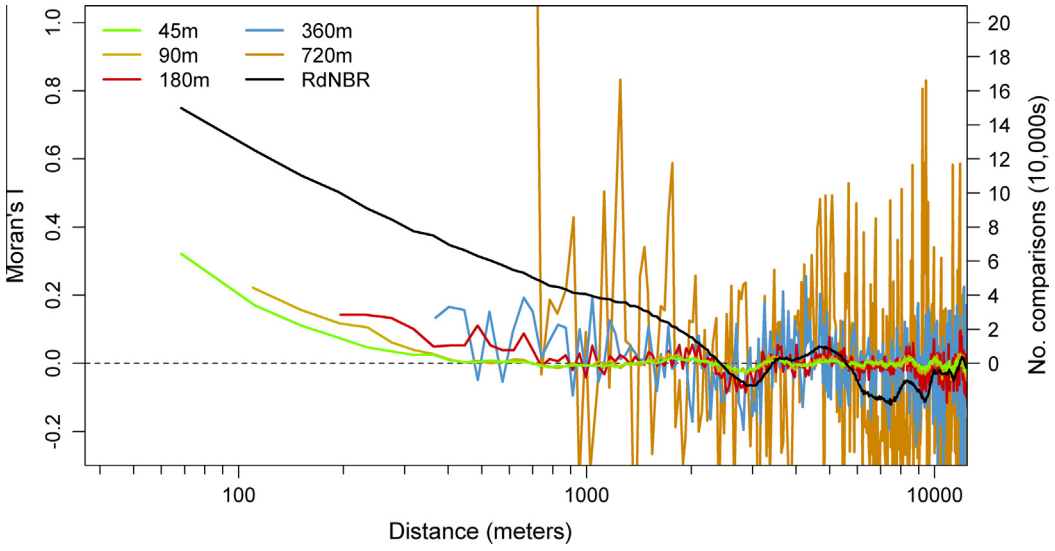

Fig. A2. Moran's *I* correlogram for out-of-bag model residuals for random forest models. Data for each model was a subsample of the full dataset based on various minimum sample spacing distances among the points. Moderate spatial autocorrelation in the residuals was present at smaller distances for all sample spacings. Rim fire RdNBR is included for reference. The number of comparisons in thousands shown on the right scale; as the distance between samples increased, the number of samples that could be compared to calculate spatial autocorrelation decreased. Note the *x*-axis is in log10 distance units. Moran's *I* values range from −1 (dispersed) to 1 (clustered), with 0 indicated completely random.

Spatial autocorrelation in fire behavior and severity may result for a variety of reasons. First, the influence of the underlying biophysical environment patterns, which itself is spatially autocorrelated at several spatial scales (Fig. A1), may contribute to SA in fire severity patterns. Second, physical properties of fire spread, such as heat transfer through convective, conductive, and radiative forces, could contribute to similar fire behavior in neighboring locations independent of local fuels, or weather conditions. Typically, under non-plume-dominated conditions, this would occur at smaller scales than our minimum sampling spacing. And finally, fine-scaled spatial autocorrelation in fire severity may also reflect patterns of localized areas where biophysical controls are stronger or weaker or where short-lived, highly localized variations in weather caused fire to burn with higher or lower severity than otherwise would be expected. A portion of the SA in our model residuals may reflect this third effect because the model fidelity to how actual burn patterns changed spatially (i.e., nonstationarity in response to fine-scaled drivers of fire severity over space and time).

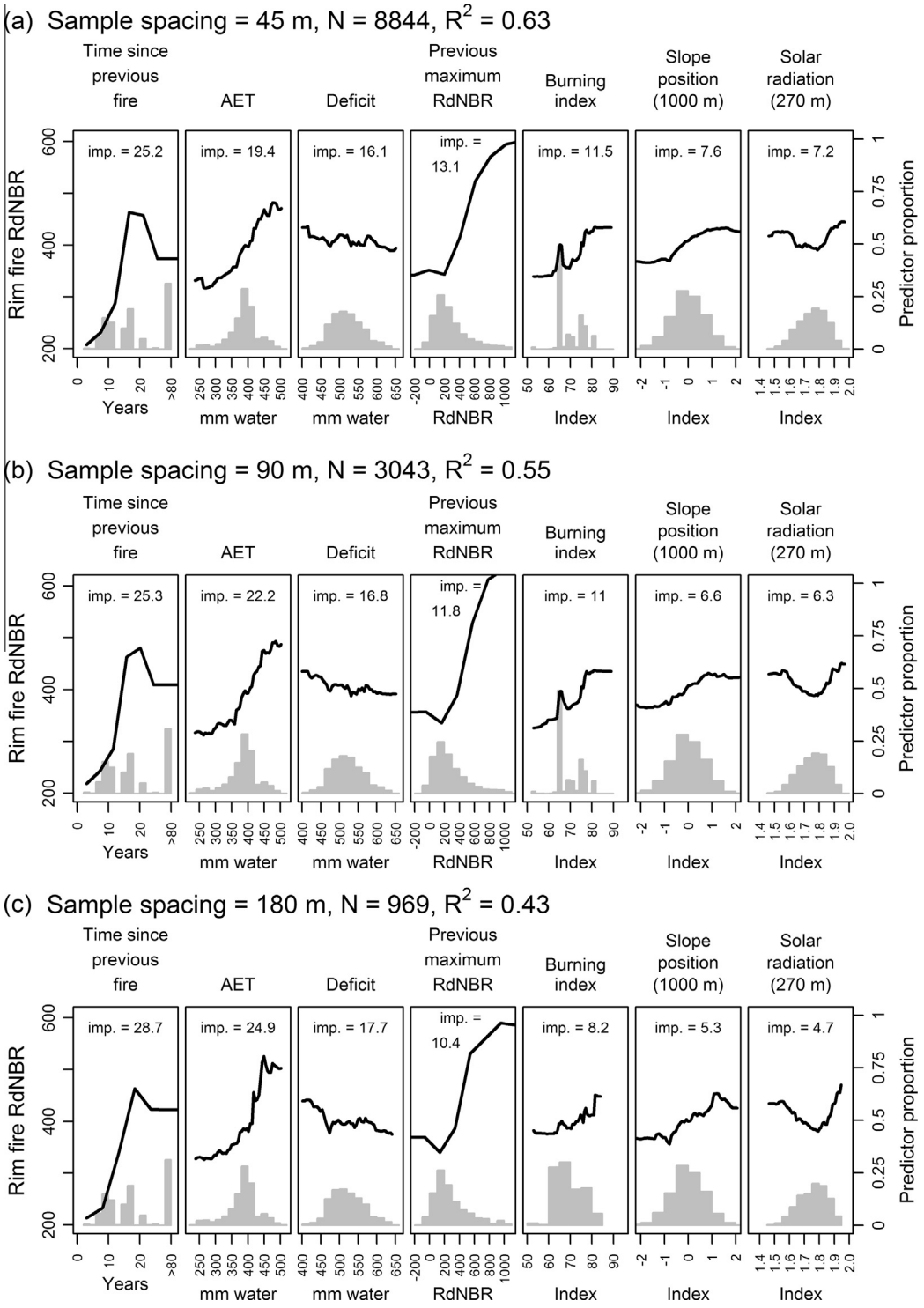

Fig. A3. Partial plots showing relationships between each of the predictors in the parsimonious predictor set and the 2013 Rim fire burn severity (RdNBR) from random forest modeling. Relationships between the predictors and RdNBR were similar and stable for sample spacing distances of 45 m (a), 90 m (b), and 180 m (c) but larger sampling distances of 360 m (d) and 720 m (e) showed model instabilities. Number within each panel shows the normalized importance of each predictor in the model ("imp. ="). Variance explained by model shown as a pseudo R^2 ("RSQ ="). Solid lines show trends in RdNBR in response to each predictor (left scale) while histograms show the distributions of values for each predictor (right scale). Model trends where there are few samples at extreme values for predictors should be treated with caution. Relationships between each predictor and the response (RdNBR) calculated as partial dependence plots where the values for each predictor are varied throughout their range while values for all other predictors are held to their mean values. As a result, partial dependence plots do not show interactions between predictors.

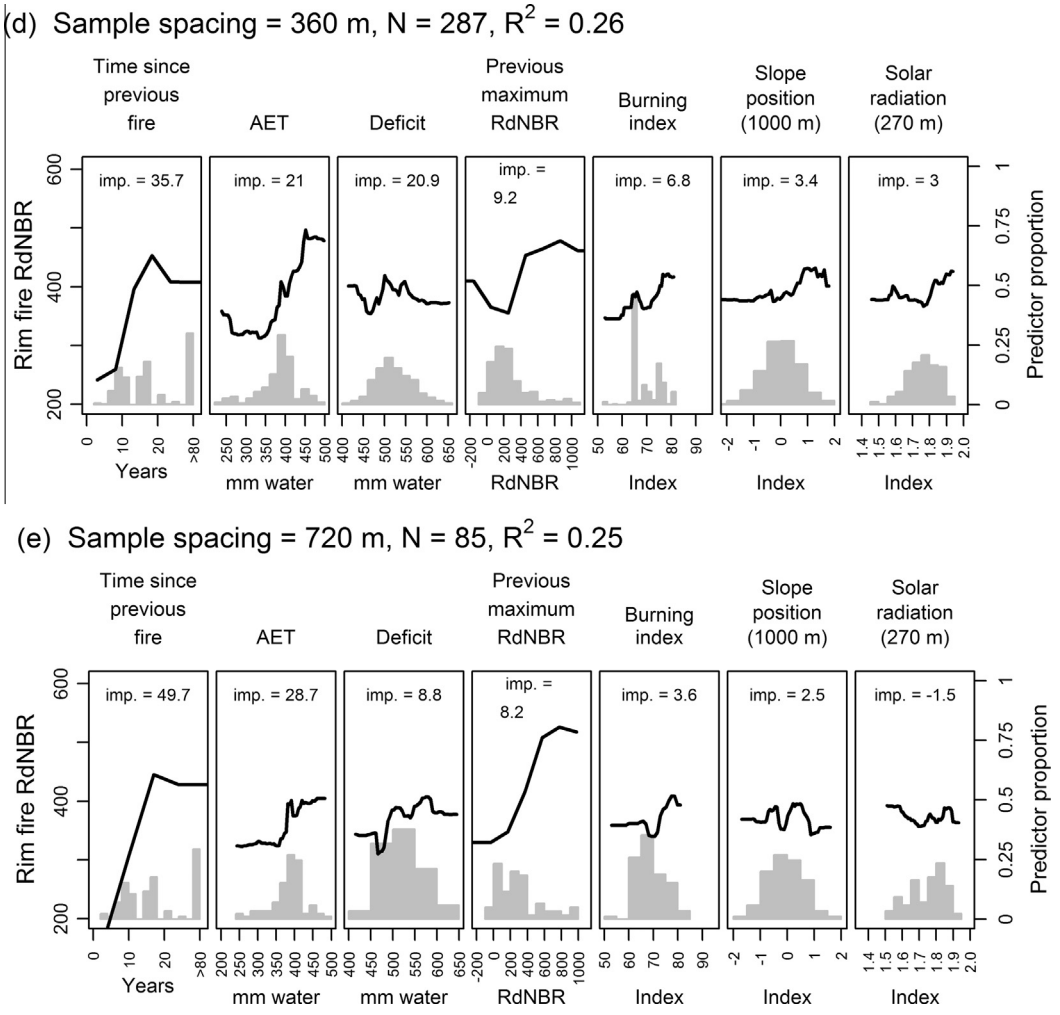

Fig. A3 (*continued*)

A.3. Random forest model results: Minimum sample spacing distances

We tested a variety of minimum sampling distances to reduce the level of spatial autocorrelation exhibited at fine scales in our data (Diniz-Filho et al., 2003). All models tested showed some autocorrelation in the residuals at smaller distances (Fig. A2). However, model residuals exhibited much lower spatial autocorrelation compared to the main predictors and RdNBR.

Models with spacing of 360 m and 720 m had poor variance explained (0.27 and 0.28, respectively) and showed oscillation in the spatial autocorrelation of their residuals. We ran our parsimonious predictor selection algorithm on each spacing sample ten times and found that spacing of 720 m, 360 m, and to a lesser degree 180 m were unstable – different sets of parsimonious predictors were selected with different runs even though the same sample set was used for each spacing. This suggested that these spacing distances were under sampling the spatial autocorrelation present in our data. Models with minimum spacing 45 m and 90 m did not have these problems. Models developed with sample distances 45 m, 90 m, and 180 m had consistent relationships between burn severity and the predictors in the parsimonious and biophysical core predictor sets (Figs. A3 and A4).

The resolution of several of the biophysical predictors AET, Deficit, and solar radiation used in the parsimonious model was 270 m – approximately one half the distance identified for residual autocorrelation in random forest model residuals (Fig. A2; 45 m and 90 m models). At this scale, spatial autocorrelation in these variables was high (Moran's *I*: ~0.77) and beginning to decrease rapidly at larger distance intervals. This suggests that either a higher-resolution biophysical variable set may provide higher fidelity predictions, or that finer-scale processes other than local climate may drive fire severity at these finer scales, which are missing from the current predictor set.

Differences in variance explained in fire severity patterns among these models may suggest that (1) closer sampling leads to better sampling of the key variations in the biophysical patterns within the study area, and/or (2) closer sample spacing simply allowed the models to pattern match fine scale heterogeneity. The former explanation could indicate that at close sample spacing, random forest models are modeling fine-scale ecological variance (desired), and the latter would indicate that models are simply matching highly similar nearby conditions (effectively overfitting; undesired). Although we cannot discount the latter explanation, we lean toward towards the former explanation because the key relationships between predictors and burn severity remained stable across ranges of sample spacing. This suggests that fine-scale, spatially autocorrelated, ecological information is important to understanding the drivers of mixed-severity burn patterns and this would be a fruitful area for future research.

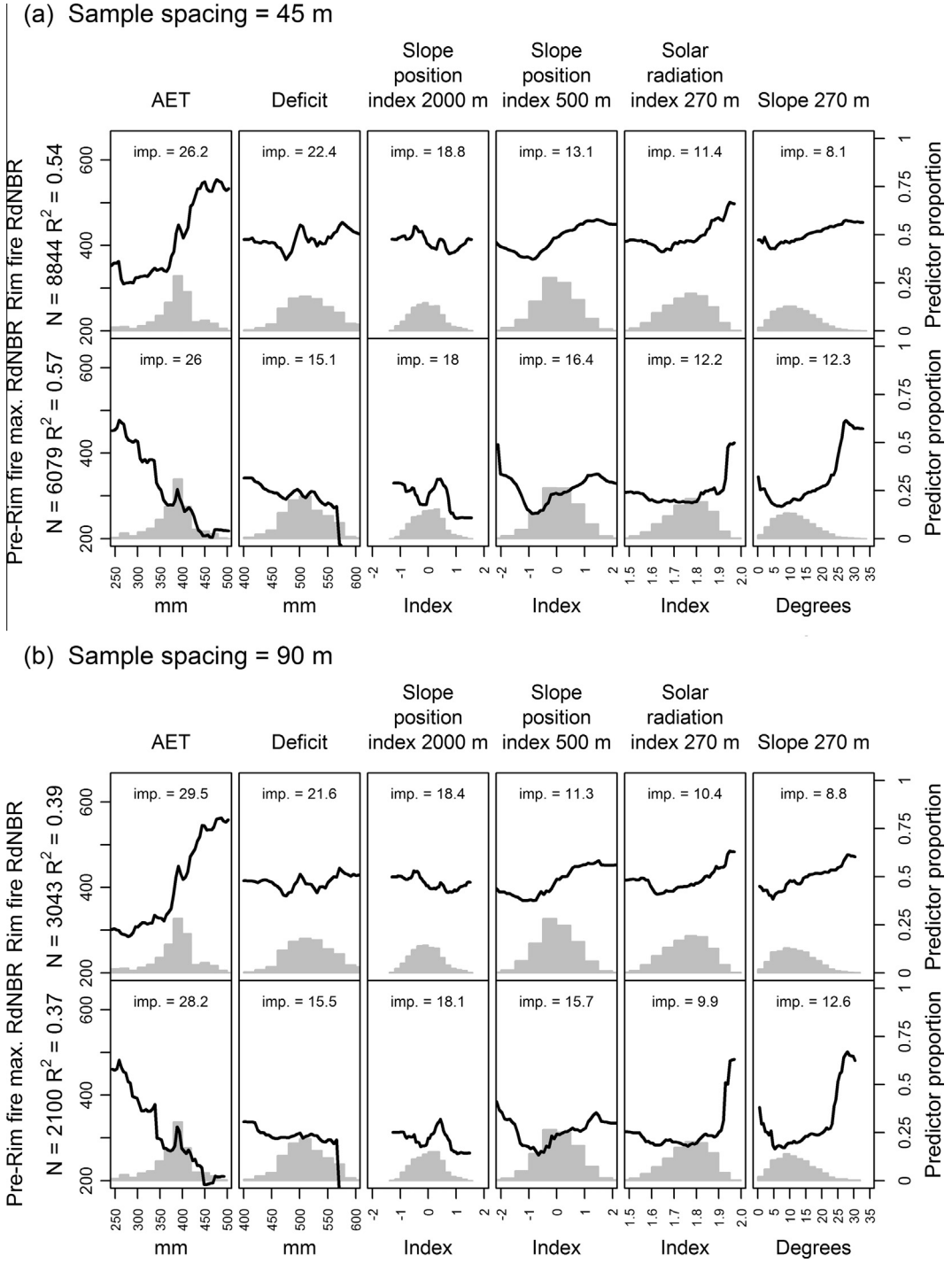

Fig. A4. Relationships between each of the predictors in the biophysical core predictor set and the 2013 Rim fire and pre-Rim fire burn severities (RdNBR) as modeled by random forest modeling. Relationships between the predictors and RdNBR were similar and stable for sample spacing distances of 45 m (a), 90 m (b), and 180 m (c) but larger sampling distances of 360 m (d) and 720 m (e) showed model instabilities. Number within each panel shows the normalized importance of each predictor in the model ("imp. ="). Variance explained by model shown as a pseudo R^2 ("RSQ ="). Solid lines show trends in RdNBR in response to each predictor (left scale) while histograms show the distributions of values for each predictor (right scale). Model trends where there are few samples at extreme values for predictors should be treated with caution. For predictors that are index values, interpretative text is included within each panel. Relationships between each predictor and the response (RdNBR) calculated as partial dependence plots where the values for each predictor are varied throughout their range while values for all other predictors are held to their mean values. As a result, partial dependence plots do not show interactions between predictors.

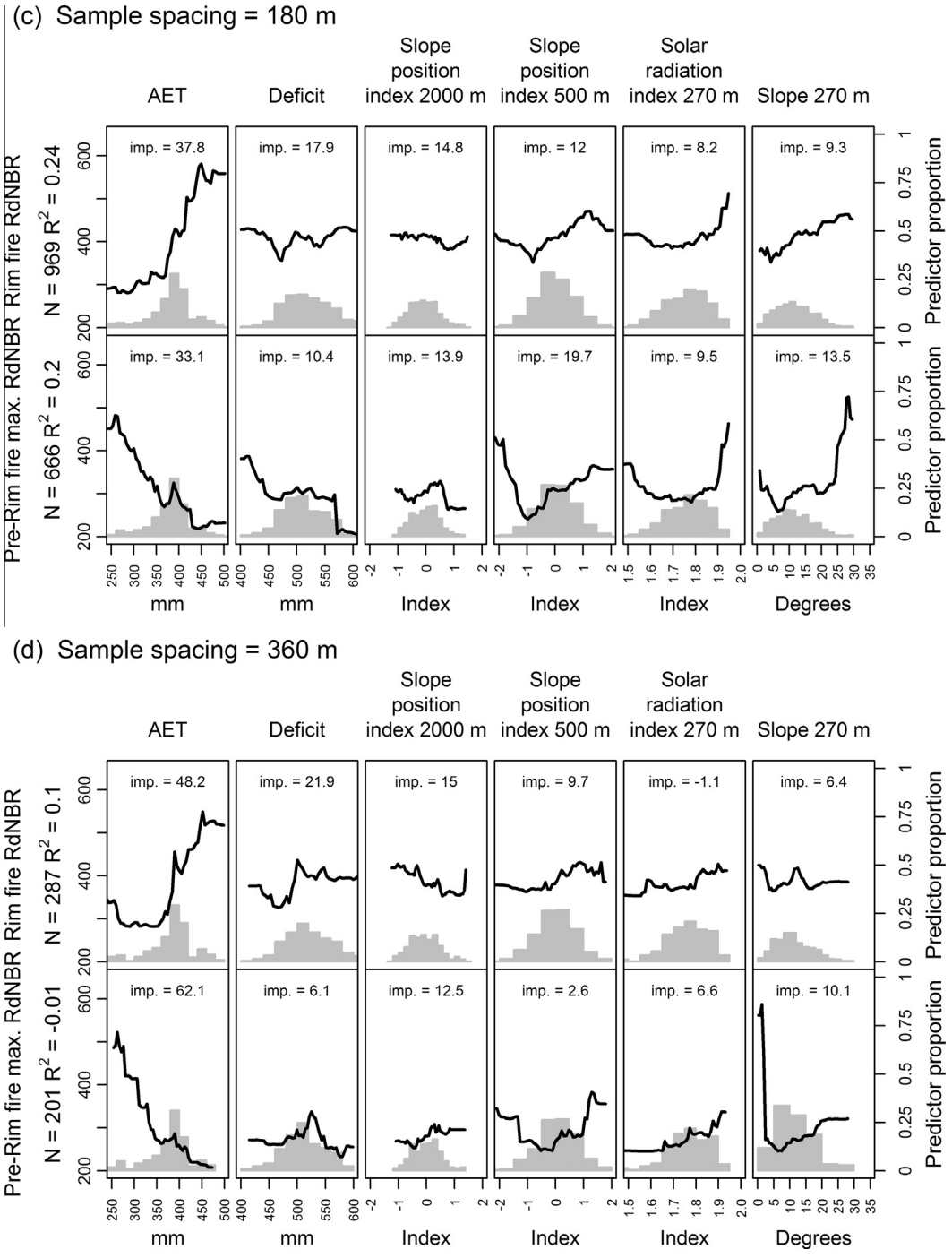

Fig. A4 (*continued*)

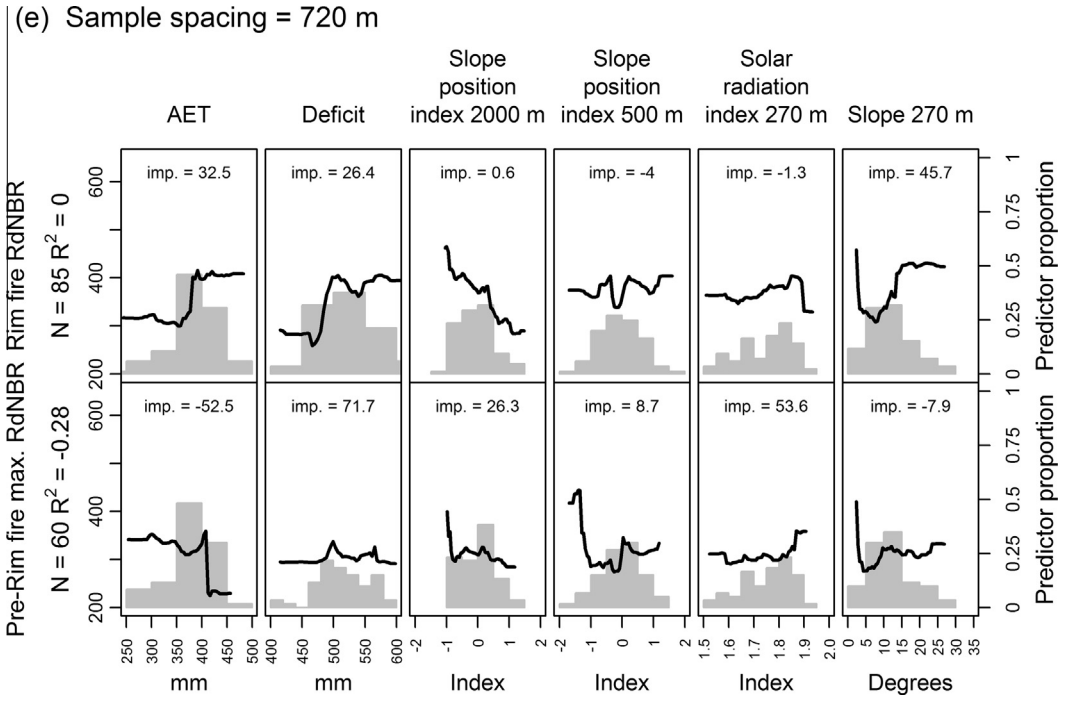

Fig. A4 (*continued*)

References

Abatzoglou, J.T., Kolden, C.A., 2013. Relationships between climate and macroscale area burned in the western United States. Int. J. Wildl. Fire 22, 1003–1020. http://dx.doi.org/10.1071/WF13019.

Beaty, R.M., Taylor, A.H., 2008. Fire history and the structure and dynamics of a mixed conifer forest landscape in the northern Sierra Nevada, Lake Tahoe Basin, California, USA. For. Ecol. Manage. 255, 707–719. http://dx.doi.org/10.1016/j.foreco.2007.09.044.

Bessie, W.C., Johnson, E.A., 1995. The relative importance of fuels and weather on fire behavior in subalpine forests. Ecology 76, 747–762. http://dx.doi.org/10.2307/1939341.

Bigler, C., Kulakowski, D., Veblen, T.T., 2005. Multiple disturbance interactions and drought influence fire severity in rocky mountain subalpine forests. Ecology 86, 3018–3029. http://dx.doi.org/10.1890/05-0011.

Bradshaw, L., Deeming, J.E., Burgan, R.E., Cohen, J.D., 1983. The 1978 National Fire-592 Danger Rating System: Technical Documentation. General Technical Report INT-169. USDA Forest Service Rocky Mountain Research Station, Ogden, UT.

Breiman, L., 2001. Random forests. Eur. J. Math. 45, 5–32. http://dx.doi.org/10.1023/A:1010933404324.

Breiman, L., Friedman, J.H., Olshen, R.A., Stone, C.J., 1984. Classification and Regression Trees. Chapman & Hall, New York.

Cansler, C.A., McKenzie, D., 2012. How robust are burn severity indices when applied in a new region? evaluation of alternate field-based and remote-sensing methods. Remote Sens. 4, 456–483. http://dx.doi.org/10.3390/rs4020456.

Cansler, C.A., McKenzie, D., 2014. Climate, fire size, and biophysical setting control fire severity and spatial pattern in the northern Cascade Range, USA. Ecol. Appl. 24, 1037–1056. http://dx.doi.org/10.1890/13-1077.1.

Churchill, D., Larson, A.J., Dahlgreen, M.C., Franklin, J.F., Hessburg, P.F., Lutz, J.A., 2013. Restoring forest resilience: from reference spatial patterns to silvicultural prescriptions and monitoring. For. Ecol. Mangae. 291, 442–457. http://dx.doi.org/10.1016/j.foreco.2012.11.007.

Clifford, P., Richardson, S., Hemon, D., 1989. Assessing the significance of the correlation between two spatial processes. Biometrics 45, 123–134.

Collins, B.M., Stephens, S.L., 2007. Managing natural wildfires in Sierra Nevada wilderness areas. Front. Ecol. Environ. 5, 523–527. http://dx.doi.org/10.1890/1540-9295(2007) 5[523:MNWISN]2.0.CO;2.

Collins, B.M., Kelly, M., Van Wagtendonk, J.W., Stephens, S.L., 2007. Spatial patterns of large natural fires in Sierra Nevada wilderness areas. Landsc. Ecol. 22, 545–557. http://dx.doi.org/10.1007/s10980-006-9047-5.

Collins, B.M., Miller, J.D., Thode, A.E., Kelly, M., van Wagtendonk, J.W., Stephens, S.L., 2009. Interactions among wildland fires in a long-established Sierra Nevada natural fire area. Ecosystems 12, 114–128. http://dx.doi.org/10.1007/s10021-008-9211-7.

Collins, B.M., Everett, R.G., Stephens, S.L., 2011. Impacts of fire exclusion and recent managed fire on forest structure in old growth Sierra Nevada mixed-conifer forests. Ecosphere 2. http://dx.doi.org/10.1890/ES11-00026.1, art51.

Cutler, D.R., Edwards, T.C., Beard, K.H., Cutler, A., Hess, K.T., Gibson, J., Lawler, J.J., 2007. Random forests for classification in ecology. Ecology 88, 2783–2792. http://dx.doi.org/10.1890/07-0539.1.

Das, A.J., Stephenson, N.L., Flint, A., Das, T., van Mantgem, P.J., 2013. Climatic correlates of tree mortality in water- and energy-limited forests. PLoS One 8, e69917. http://dx.doi.org/10.1371/journal.pone.0069917.

Dillon, G.K., Holden, Z.A., Morgan, P., Crimmins, M.a., Heyerdahl, E.K., Luce, C.H., 2011. Both topography and climate affected forest and woodland burn severity in two regions of the western US, 1984 to 2006. Ecosphere 2. http://dx.doi.org/10.1890/ES11-00271.1, art130.

Diniz-Filho, J.A.F., Bini, L.M., Hawkins, B.A., 2003. Spatial autocorrelation and red herrings in geographical ecology. Global Ecol. Biogeogr. 12, 53–64.

Dormann, C.F., McPherson, J.M., Araújo, M.B., Bivand, R., Bolliger, J., Carl, G., Davies, R.G., Hirzel, A., Jetz, W., Kissling, W.D., Kühn, I., Ohlemüller, R., Peres-Neto, P.R., Reineking, B., Schröder, B., Schurr, F.M., Wilson, R., 2007. Methods to account for spatial autocorrelation in the analysis of species distributional data: a review. Ecography 30, 609–628.

Dubin, R.A., 1998. Spatial autocorrelation: a primer. J. Housing Econ. 7, 304–327.

Eidenshink, J., Schwind, B., Brewer, K., Zhu, Z., Quayle, B., Howard, S., 2007. A project for monitoring trends in burn severity. Fire Ecol. 3 (1), 3–21. http://dx.doi.org/10.4996/fireecology.0301003.

Falk, D.A., Miller, C., McKenzie, D., Black, A.E., 2007. Cross-scale analysis of fire regimes. Ecosystems 10, 809–823.

Finney, M.A.(, 2005. The challenge of quantitative risk analysis for wildland fire. For. Ecol. Manage. 211 (1–2), 97–108. http://dx.doi.org/10.1016/j.foreco.2005.02.010.

Flint, L.E., Flint, A.L., 2007. Regional analysis of ground-water recharge. Ground-water Recharg. Arid semiarid Southwest, United States, 29–59.

Flint, L.E., Flint, A.L., Thorne, J.H., Boynton, R., 2013. Fine-scale hydrologic modeling for regional landscape applications: the California Basin Characterization Model development and performance. Ecol. Process. 2, 25. http://dx.doi.org/10.1186/2192-1709-2-25.

Gill, L., Taylor, A.H., 2009. Top-down and bottom-up controls on fire regimes along an elevational gradient on the east slope of the Sierra Nevada, California, USA. Fire Ecol. 5, 57–75. http://dx.doi.org/10.4996/fireecology.0503057.

Gillett, N.P., Weaver, A.J., Zwiers, F.W., Flannigan, M.D., 2004. Detecting the effect of climate change on Canadian forest fires. Geophys. Res. Lett. 31. http://dx.doi.org/10.1029/2004GL020876.

Greenberg, J.A., Dobrowski, S.Z., Vanderbilt, V.C., 2009. Limitations on maximum tree density using hyperspatial remote sensing and environmental gradient analysis. Remote Sens. Environ. 113, 94–101. http://dx.doi.org/10.1016/j.rse.2008.08.014.

Halofsky, J.E., Donato, D.C., Hibbs, D.E., Campbell, J.L., Cannon, M.D., Fontaine, J.B., Thompson, J.R., Anthony, R.G., Bormann, B.T., Kayes, L.J., Law, B.E., Peterson, D.L., Spies, T.A., 2011. Mixed-severity fire regimes: lessons and hypotheses from the Klamath-Siskiyou Ecoregion. Ecosphere 2. http://dx.doi.org/10.1890/ES10-00184.1, art40.

Harris, L., Taylor, A.H., 2015. Topography, fuels, and fire exclusion drive fire severity of the Rim Fire in an old-growth mixed-conifer forest, Yosemite Natioanl Park, USA. Ecosystems. http://dx.doi.org/10.1007/s10021-015-9890-9.
Hastie, T., Tibshirani, R., Friedman, J., Franklin, J., 2001. The Elements of Statistical Learning: Data Mining, Inference, and Prediction. Springer Series in Statistics. Springer, New York.
Hawkins, B.A., Diniz-Filho, J.A.F., Mauricio Bini, L., De Marco, P., Blackburn, T.M., 2007. Red herrings revisited: spatial autocorrelation and parameter estimation in geographical ecology. Ecography 30, 375–384.
Hessburg, P.F., Churchill, D.J., Larson, A.J., Haugo, R.D., Miller, C., Spies, T.A., North, M.P., Povak, N.A., Belote, R.T., Singleton, P.H., Gaines, W.L., Keane, R.E., Aplet, G. H., Stephens, S.L., Morgan, P., Bission, P.A., Rieman, B.E., Salter, R.B., Reeves, G.H., 2015. Restoring fire-prone Inland Pacific landscapes: seven core principles. Landsc. Ecol. 1–31. http://dx.doi.org/10.1007/s10980-015-0218-0.
Heyerdahl, E.K., Brubaker, L.B., Agee, J.K., 2001. Spatial controls of historical fire regimes: a multiscale example from the interior west, USA. Ecology 82, 660–678. http://dx.doi.org/10.1890/0012-9658(2001) 082[0660:SCOHFR]2.0.CO;2.
Holden, Z.A., Morgan, P., Evans, J.S., 2009. A predictive model of burn severity based on 20-year satellite-inferred burn severity data in a large southwestern US wilderness area. For. Ecol. Manage. 258, 2399–2406. http://dx.doi.org/10.1016/j.foreco.2009.08.017.
Hothorn, T., Müller, J., Schröder, B., Kneib, T., Brandl, R., 2011. Decomposing environmental, spatial, and spatiotemporal components of species distributions. Ecol. Monogr. 81, 329–347.
Jakubowksi, M.K., Guo, Q., Collins, B., Stephens, S., Kelly, M., 2013. Predicting surface fuel models and fuel metrics using Lidar and CIR imagery in a dense, mountainous forest. Photogramm. Eng. Remote Sensing 79, 37–49. http://dx.doi.org/10.14358/PERS.79.1.37.
Jenness, J., 2006. Topographic Position Index (tpi_jen. avx) extension for ArcView 3. x, v. 1.3 a. Jenness Enterprises.
Kane, V.R., Lutz, J.A., Roberts, S.L., Smith, D.F., McGaughey, R.J., Povak, N.A., Brooks, M.L., 2013. Landscape-scale effects of fire severity on mixed-conifer and red fir forest structure in Yosemite National Park. For. Ecol. Manage. 287, 17–31. http://dx.doi.org/10.1016/j.foreco.2012.08.044.
Kane, V.R., North, M.P., Lutz, J.A., Churchill, D.J., Roberts, S.L., Smith, D.F., McGaughey, R.J., Kane, J.T., Brooks, M.L., 2014. Assessing fire effects on forest spatial structure using a fusion of Landsat and airborne LiDAR data in Yosemite National Park. Remote Sens. Environ. 151, 89–101. http://dx.doi.org/10.1016/j.rse.2013.07.041.
Kane, V.R., Lutz, J.A., Alina Cansler, C., Povak, N.A., Churchill, D.J., Smith, D.F., Kane, J. T., North, M.P., 2015. Water balance and topography predict fire and forest structure patterns. For. Ecol. Manage. 338, 1–13. http://dx.doi.org/10.1016/j.foreco.2014.10.038.
Keane, R.E., Gray, K., Bacciu, V., 2012a. Spatial Variability of Wildland Fuel Characteristics in Northern Rocky Mountain Ecosystems. Fort Collins, CO.
Keane, R.E., Gray, K., Bacciu, V., Leirfallom, S., 2012b. Spatial scaling of wildland fuels for six forest and rangeland ecosystems of the northern Rocky Mountains, USA. Landsc. Ecol. 27, 1213–1234. http://dx.doi.org/10.1007/s10980-012-9773-9.
Keating, K.A., Gogan, P.J.P., Vore, J.M., Irby, L.R., 2007. A simple solar radiation index for wildlife habitat studies. J. Wildl. Manage. 71, 1344–1348. http://dx.doi.org/10.2193/2006-359.
Keeler-Wolf, T., Moore, P.E., Reyes, E.T., Menke, J.M., Johnson, D.N., Karavidas, D.L., 2012. Yosemite National Park Vegetation Classification and Mapping Project Report. Natural Resource Report NPS/YOSE/NRTR-2012/598.
Larson, A.J., Churchill, D., 2012. Tree spatial patterns in fire-frequent forests of western North America, including mechanisms of pattern formation and implications for designing fuel reduction and restoration treatments. For. Ecol. Manage. 267, 74–92. http://dx.doi.org/10.1016/j.foreco.2011.11.038.
Larson, A.J., Travis Belote, R., Alina Cansler, C., Parks, S.A., Dietz, M.S., 2013. Latent resilience in ponderosa pine forest: effects of resumed frequent fire. Ecol. Appl. 23, 1243–1249. http://dx.doi.org/10.1890/13-0066.1.
Lee, S.-W.W., Lee, M.-B.B., Lee, Y.-G.G., Won, M.-S.S., Kim, J.-J.J., Hong, S.K., 2009. Relationship between landscape structure and burn severity at the landscape and class levels in Samchuck, South Korea. For. Ecol. Manage. 258, 1594–1604. http://dx.doi.org/10.1016/j.foreco.2009.07.017.
Legendre, P., 1993. Spatial autocorrelation: trouble or new paradigm? Ecology 74, 1659–1673.
Legendre, P., Legendre, L.F.J., 2012. Numerical Ecology, third ed. Elsevier, Amsterdam, The Netherlands.
Lennon, J.J., 2000. Red-shifts and red herrings in geographical ecology. Ecography 23 (1), 101–113.
Lertzman, K., Fall, J., 1998. From forest stands to landscapes: spatial scales and the roles of disturbances. In: Ecological Scale: Theory and Applications. Columbia University Press, New York, pp. 339–367, TS – RIS.
Littell, J.S., Gwozdz, R.B., 2011. Climatic water balance and regional fire years in the Pacific Northwest, USA: linking regional climate and fire at landscape scales. In: McKenzie, D., Miller, C., Falk, D.A. (Eds.), The Landscape Ecology of Fire. Springer, New York.
Lutz, J.A., van Wagtendonk, J.W., Thode, A.E., Miller, J.D., Franklin, J.F., 2009. Climate, lightning ignitions, and fire severity in Yosemite National Park, California, USA. Int. J. Wildl. Fire 18, 765–774. http://dx.doi.org/10.1071/WF08117.
Lutz, J.A., van Wagtendonk, J.W., Franklin, J.F., 2010. Climatic water deficit, tree species ranges, and climate change in Yosemite National Park. J. Biogeogr. 37, 936–950. http://dx.doi.org/10.1111/j.1365-2699.2009.02268.x.
Lutz, J.A., Key, C.H., Kolden, C.A., Kane, J.T., van Wagtendonk, J.W., 2011. Fire frequency, area burned, and severity: a quantitative approach to defining a normal fire year. Fire Ecol. 7, 51–65. http://dx.doi.org/10.4996/fireecology.0702051.
Lydersen, J., North, M., 2012. Topographic variation in structure of mixed-conifer forests under an active-fire regime. Ecosystems 15, 1134–1146. http://dx.doi.org/10.1007/s10021-012-9573-8.
Lydersen, J.M., North, M.P., Collins, B.M., 2014. Severity of an uncharacteristically large wildfire, the Rim Fire, in forests with relatively restored frequent fire regimes. For. Ecol. Manage. 328, 326–334. http://dx.doi.org/10.1016/j.foreco.2014.06.005.
Lydersen, J.M., Collins, B.M., Knapp, E.E., Roller, G.B., Stephens, S., 2015. Relating fuel loads to overstorey structure and composition in a fire-excluded Sierra Nevada mixed conifer forest. Int. J. Wildl. Fire.
Mallek, C., Safford, H., Viers, J., Miller, J., 2013. Modern departures in fire severity and area vary by forest type, Sierra Nevada and southern Cascades, California, USA. Ecosphere 4, 1–28. http://dx.doi.org/10.1890/ES13-00217.
McGaughey, R.J., 2014. FUSION/LDV: Software for LiDAR Data Analysis and Visualization Version 3.42.
McKenzie, D., Kennedy, M., 2011. Scaling laws and complexity in fire regimes. In: McKenzie, D., Miller, C., Falk, D.A. (Eds.), 2011 The Landscape Ecology of Fire, vol. 213. Springer Science & Business Media (Chapter 2).
Miller, J.D., Safford, H., 2012. Trends in wildfire severity: 1984 to 2010 in the Sierra Nevada, Modoc Plateau, and southern Cascades, California, USA. Fire Ecol. 8, 41–57. http://dx.doi.org/10.4996/fireecology.0803041.
Miller, J.D., Thode, A.E., 2007. Quantifying burn severity in a heterogeneous landscape with a relative version of the delta Normalized Burn Ratio (dNBR). Remote Sens. Environ. 109, 66–80. http://dx.doi.org/10.1016/j.rse.2006.12.006.
Miller, C., Urban, D.L., 1999. A model of surface fire, climate and forest pattern in the Sierra Nevada, California. Ecol. Modell. 114, 113–135. http://dx.doi.org/10.1016/S0304-3800(98)00119-7.
Miller, C., Urban, D.L., 2000. Connectivity of forest fuels and surface fire regimes. Landsc. Ecol. 15, 145–154. http://dx.doi.org/10.1023/A:1008181313360.
Miller, J.D., Safford, H.D., Crimmins, M., Thode, A.E., 2009a. Quantitative evidence for increasing forest fire severity in the Sierra Nevada and Southern Cascade Mountains, California and Nevada, USA. Ecosystems 12, 16–32. http://dx.doi.org/10.1007/s10021-008-9201-9.
Miller, J.D., Knapp, E.E., Key, C.H., Skinner, C.N., Isbell, C.J., Creasy, R.M., Sherlock, J. W., 2009b. Calibration and validation of the relative differenced Normalized Burn Ratio (RdNBR) to three measures of fire severity in the Sierra Nevada and Klamath Mountains, California, USA. Remote Sens. Environ. 113, 645–656. http://dx.doi.org/10.1016/j.rse.2008.11.009.
Miller, J.D., Collins, B.M., Lutz, J.A., Stephens, S.L., van Wagtendonk, J.W., Yasuda, D. A., 2012a. Differences in wildfires among ecoregions and land management agencies in the Sierra Nevada region, California, USA. Ecosphere 3 (9), 80. http://dx.doi.org/10.1890/ES12-00158.1.
Miller, J.D., Skinner, C.N., Safford, H.D., Knapp, E.E., Ramirez, C.M., 2012b. Trends and causes of severity, size, and number of fires in northwestern California, USA. Ecol. Appl. 22, 184–203. http://dx.doi.org/10.1890/10-2108.1.
Morgan, P., Heyerdahl, E.K., Gibson, C.E., 2008. Multi-season climate synchronized forest fires throughout the 20th century, northern Rockies, USA. Ecology 89, 717–728. http://dx.doi.org/10.1890/06-2049.1.
Mu, Q., Heinsch, F.A., Zhao, M., Running, S.W., 2007. Development of a global evapotranspiration algorithm based on MODIS and global meteorology data. Remote Sens. Environ. 111, 519–536. http://dx.doi.org/10.1016/j.rse.2007.04.015.
North, M. Stine, P., O'Hara, K., Zielinski, W., Stephens, S., 2009. An ecosystem management strategy for Sierran mixed-conifer forests. Gen. Tech. Rep. PSW-GTR-220. U.S. Department of Agriculture, Forest Service, Pacific Southwest Research Station, Albany, CA.
North, M., Brough, A., Long, J., Collins, B., Bowden, P., Yasuda, D., Miller, J., Sugihara, N., 2015. Constraints on mechanized treatment significantly limit mechanical fuels reduction extent in the Sierra Nevada. J. For. 113, 40–48. http://dx.doi.org/10.5849/jof.14-058.
Parks, S.A., Parisien, M.A., Miller, C., 2011. Multi-scale evaluation of the environmental controls on burn probability in a southern Sierra Nevada landscape. Int. J. Wildl. Fire 20, 815–828. http://dx.doi.org/10.1071/WF10051.
Parks, S.A., Parisien, M.A., Miller, C., 2012. Spatial bottom-up controls on fire likelihood vary across western North America. Ecosphere 3. http://dx.doi.org/10.1890/ES11-00298.1, art12.
Parks, S.A., Miller, C., Nelson, C.R., Holden, Z.A., 2014a. Previous fires moderate burn severity of subsequent wildland fires in two large western US wilderness areas. Ecosystems 17, 29–42. http://dx.doi.org/10.1007/s10021-013-9704-x.
Parks, S.A., Parisien, M.A., Miller, C., Dobrowski, S.Z., 2014b. Fire activity and severity in the western US vary along proxy gradients representing fuel amount and fuel moisture. PLoS One 9, e99699. http://dx.doi.org/10.1371/journal.pone.0099699.
Parks, S.A., Holsinger, L.M., Miller, C., Nelson, C.R., 2015. Wildland fire as a self-regulating mechanism: the role of previous burns and weather in limiting fire progression. Ecol. Appl. 150203154931002. http://dx.doi.org/10.1890/14-1430.1.
Perry, D.A., Hessburg, P.F., Skinner, C.N., Spies, T.A., Stephens, S.L., Taylor, A.H., Franklin, J.F., McComb, B., Riegel, G., 2011. The ecology of mixed severity fire regimes in Washington, Oregon, and Northern California. For. Ecol. Manage. 262, 703–717. http://dx.doi.org/10.1016/j.foreco.2011.05.004.

Peterson, G.D., 2002. Contagious disturbance, ecological memory, and the emergence of landscape pattern. Ecosystems 5, 329–338.
Prichard, S.J., Kennedy, M.C., 2014. Fuel treatments and landform modify landscape patterns of burn severity in an extreme fire event. Ecol. Appl. 24, 571–590. http://dx.doi.org/10.1890/13-0343.1.
Priestley, C.H.B., Taylor, R.J., 1972. On the assessment of surface heat flux and evaporation using large-scale parameters. Mon. Weather Rev. 100, 81–92. http://dx.doi.org/10.1175/1520-0493(1972) 100<0081:OTAOSH>2.3.CO;2.
Schoennagel, T., Veblen, T.T., Romme, W.H., Sibold, J.S., Cook, E.R., 2005. ENSO and PDO variability affect drought-induced fire occurrence in rocky mountain subalpine forests. Ecol. Appl. 15, 2000–2014. http://dx.doi.org/10.1890/04-1579.
Scholl, A.E., Taylor, A.H., 2010. Fire regimes, forest change, and self-organization in an old-growth mixed-conifer forest, Yosemite National Park, USA. Ecol. Appl. 20, 362–380. http://dx.doi.org/10.1890/08-2324.1.
Smith, A.M.S., Kolden, C.A., Tinkham, W.T., Talhelm, A.F., Marshall, J.D., Hudak, A.T., Boschetti, L., Falkowski, M.J., Greenberg, J.A., Anderson, J.W., Kliskey, A., Alessa, L., Keefe, R.F., Gosz, J.R., 2014. Remote sensing the vulnerability of vegetation in natural terrestrial ecosystems. Remote Sens. Environ. 154, 322–337.
Soverel, N.O., Perrakis, D.D.B., Coops, N.C., 2010. Estimating burn severity from Landsat dNBR and RdNBR indices across western Canada. Remote Sens. Environ. 114, 1896–1909. http://dx.doi.org/10.1016/j.rse.2010.03.013.
Stephenson, N.L., 1998. Actual evapotranspiration and deficit: biologically meaningful correlates of vegetation distribution across spatial scales. J. Biogeogr. 25, 855–870. http://dx.doi.org/10.1046/j.1365-2699.1998.00233.x.
Sugihara, N., van Wagtendonk, J.W., Fites-Kaufman, J., Shaffer, K., Thode, A.E., 2006a. The future of fire in California's ecosystems. In: Sugihara, N.G., van Wagtendonk, J.W., Shaffer, K.E., Fites-Kaufman, J.T.A.E. (Eds.), Fire in California's Ecosystems. University of California Press, Berkely, CA, USA, pp. 538–544.
Sugihara, N.G., van Wagtendonk, J.W., Fites-Kaufman, J., 2006b. Fire as an ecological process. In: Sugihara, N.G., van Wagtendonk, J.W., Shaffer, K.E., Fites-Kaufman, J. T.A.E. (Eds.), Fire in California's Ecosystems. University of California Press, Berkely, CA, USA, pp. 58–74.
Taylor, A.H., Skinner, C.N., 1998. Fire history and landscape dynamics in a late-successional reserve, Klamath Mountains, California, USA. For. Ecol. Manage. 111, 285–301. http://dx.doi.org/10.1016/S0378-1127(98)00342-9.
Thode, A.E., 2005. Quantifying the Fire Regime Attributes of Severity and Spatial Complexity using Field and Imagery Data. University of California, Davis, CA.
Thode, A.E., Van Wagtendonk, J.W., Miller, J.D., Quinn, J.F., 2011. Quantifying the fire regime distributions for severity in Yosemite National Park, California, USA. Int. J. Wildl. Fire 20, 223–239. http://dx.doi.org/10.1071/WF09060.
Thompson, J.R., Spies, T.A., Ganio, L.M., 2007. Reburn severity in managed and unmanaged vegetation in a large wildfire. Proc. Natl. Acad. Sci. USA 104, 10743–10748. http://dx.doi.org/10.1073/pnas.0700229104.
Thornthwaite, C.W., Mather, J.R., 1955. The water balance. Publ. Climatol. 8, 1–104.
Tobler, W.R., 1970. A computer movie simulating urban growth in the Detroit region. Econ. Geogr. 46, 234–240.
Turner, M.G., Romme, W.H., 1994. Landscape dynamics in crown fire ecosystems. Landsc. Ecol. 9, 59–77. http://dx.doi.org/10.1007/bf00135079.
Van de Water, K.M., Safford, H., 2011. A summary of fire frequency estimates for California vegetation before Euro-American settlement. Fire Ecol. 7 (3), 26–58. http://dx.doi.org/10.4996/fireecology.0703026.
van Wagtendonk, J.W., 2007. The history and evolution of wildland fire use. Fire Ecol. 3 (2), 3–17. http://dx.doi.org/10.4996/fireecology.0302003.
van Wagtendonk, J.W., Fites-Kaufman, J., 2006. Sierra Nevada bioregion. In: Sugihara, N.G., van Wagtendonk, J.W., Shaffer, K.E., Fites-Kaufman, J.T.A.E. (Eds.), Fire in California's Ecosystems. University of California Press, Berkely, CA, USA, pp. 264–294.
van Wagtendonk, J.W., Lutz, J.A., 2007. Fire regime attributes of wildland fires in Yosemite National Park, USA. Fire Ecol. 3 (2), 34–52. http://dx.doi.org/10.4996/fireecology.0302034.
van Wagtendonk, J.W., Moore, P.E., 2010. Fuel deposition rates of montane and subalpine conifers in the central Sierra Nevada, California, USA. For. Ecol. Manage. 259, 2122–2132. http://dx.doi.org/10.1016/j.foreco.2010.02.024.
van Wagtendonk, J.W., van Wagtendonk, K.A., Thode, A.E., 2012. Factors associated with the severity of intersecting fires in Yosemite National Park, California, USA. Fire Ecol. 8 (1), 11–31. http://dx.doi.org/10.4996/fireecology.0801011.
Walker, R.E., 2000. Investigations in Vegetation Map Rectification, and the Remotely Sensed Detection and Measurement of Natural Vegetation Changes. University of California Santa Barbara, Santa Barbara, CA.
Weiss, A., 2001. Topographic position and landforms analysis. In: Poster Presentation, ESRI User Conference, San Diego, CA.
Westerling, A.L., Hidalgo, H.G., Cayan, D.R., Swetnam, T.W., 2006. Warming and earlier spring increase western U.S. forest wildfire activity. Science 313, 940–943. http://dx.doi.org/10.1126/science.1128834.
Wieslander, A.E., 1935. A vegetation type map of California. Madroño 3, 140–144.
Wimberly, M.C., Cochrane, M.A., Baer, A.D., Pabst, K., 2009. Assessing fuel treatment effectiveness using satellite imagery and spatial statistics. Ecol. Appl. 19, 1377–1384. http://dx.doi.org/10.1890/08-1685.1.
Zevenbergen, L.W., Thorne, C.R., 1987. Quantitative analysis of land surface topography. Earth Surf. Process. Landforms 12, 47–56. http://dx.doi.org/10.1002/esp.3290120107.